



1                                    Seasonal Analysis of Reduced and Oxidized Nitrogen-Containing  
2                                    Organic Compounds at a Coastal Site

3                                    Jenna C. Ditto<sup>1,†</sup>, Jo Machesky<sup>1</sup>, and Drew R. Gentner<sup>1,\*</sup>

4                                    <sup>1</sup> Department of Chemical and Environmental Engineering, Yale University,  
5                                    New Haven, CT, 06511, USA

6                                    <sup>†</sup> Now at: Department of Chemical Engineering and Applied Chemistry, University of Toronto,  
7                                    Toronto, ON, M5S 3E5, Canada

8                                    \* Correspondence to: [drew.gentner@yale.edu](mailto:drew.gentner@yale.edu)

9  
10 **Abstract**

11                                    Nitrogen-containing organic compounds, which may be directly emitted to the  
12                                    atmosphere or may form via reactions with prevalent reactive nitrogen species (e.g. NH<sub>3</sub>, NO<sub>x</sub>,  
13                                    NO<sub>3</sub>), have important but uncertain effects on climate and human health. Using gas and liquid  
14                                    chromatography with soft ionization and high-resolution mass spectrometry, we performed a  
15                                    molecular-level speciation of functionalized organic compounds at a coastal site on the Long  
16                                    Island Sound in summer (during the LISTOS 2018 campaign) and winter. This region often  
17                                    experiences poor air quality due to the emissions of reactive anthropogenic, biogenic, and  
18                                    marine-derived compounds and their chemical transformation products. Indeed, we observed a  
19                                    range of functionalized compounds containing oxygen, nitrogen, and/or sulfur atoms resulting  
20                                    from a mix of direct emissions and chemical transformations, including photochemical  
21                                    processing in summer and aqueous-phase processing in winter. In both summer and winter,  
22                                    nitrogen-containing organic aerosols dominated the observed distribution of functionalized  
23                                    particle-phase species ionized by our analytical techniques, with 85% and 68% of measured



24 compound abundance containing a nitrogen atom, respectively. Nitrogen-containing particles  
25 included reduced nitrogen functional groups (e.g. amines, imines, azoles) and common  $\text{NO}_z$   
26 contributors (e.g. organonitrates). The prevalence of reduced nitrogen functional groups  
27 observed in the particle-phase, while frequently paired with oxygen-containing groups elsewhere  
28 on the molecule, often rivaled that of oxidized nitrogen groups detected by our methods.  
29 Supplemental gas-phase measurements, collected on adsorptive samplers and analyzed with a  
30 novel liquid chromatography-based method, suggest that gas-phase reduced nitrogen compounds  
31 are possible contributing precursors to the observed nitrogen-containing particles. Altogether,  
32 this work highlights the prevalence of reduced nitrogen-containing compounds in the less-  
33 studied Northeastern U.S., and potentially in other regions with similar anthropogenic, biogenic,  
34 and marine source signatures.

35

## 36 **1. Introduction**

37 Coastal regions near the Long Island Sound often experience poor air quality due to a  
38 combination of biogenic and anthropogenic emissions from upwind metropolitan areas along the  
39 East Coast of the U.S. It is well established that these emissions undergo chemical  
40 transformations to form secondary pollutants during hours to days of over-water transport to  
41 downwind locations, including the states of Connecticut, Rhode Island, and Massachusetts (e.g.  
42 Cleveland et al., 1976). Emissions of gas-phase organic compounds (e.g. volatile, intermediate,  
43 and semi-volatile organic compounds (VOCs, IVOCs, SVOCs)) and primary organic aerosols  
44 (POA) are oxidized via numerous pathways in the atmosphere to yield ozone ( $\text{O}_3$ ) and secondary  
45 organic aerosol (SOA) (Hallquist et al., 2009). SOA constitutes a variable but significant fraction  
46 of particulate matter with a diameter of  $2.5 \mu\text{m}$  or less (i.e.  $\text{PM}_{2.5}$ ). Both  $\text{O}_3$  and  $\text{PM}_{2.5}$  are of



47 particular concern for human health and climate; O<sub>3</sub> is known to cause an increase in respiratory-  
48 related illnesses (Di et al., 2017; Jerrett et al., 2009), while PM<sub>2.5</sub> is known to cause adverse  
49 cardiovascular, respiratory, and cognitive effects and to impact climate forcings (Di et al., 2017;  
50 Hallquist et al., 2009; Kilian and Kitazawa, 2018; Pope and Dockery, 2006). Coupled with local  
51 emissions and chemistry, these incoming aged air parcels from coastal metropolitan areas  
52 contribute to the Long Island Sound region often entering nonattainment for O<sub>3</sub> (United States  
53 Environmental Protection Agency, 2020), especially in the summer.

54         The chemistry and composition of organic compound emissions and secondary  
55 transformation products in the Long Island Sound area is historically understudied, though some  
56 past work has advanced our understanding of important sources and chemical pathways in the  
57 region. For example, VOC and sub-micron particulate matter composition were investigated  
58 during the 2002 New England Air Quality Study (de Gouw et al., 2005), with further VOC  
59 speciation in 2004 during the New England Air Quality Study – Intercontinental Transport and  
60 Chemical Transformation campaign (Warneke et al., 2007). More recently, a 2015 aircraft  
61 campaign in the Northeast U.S. called WINTER characterized wintertime chemistry in the region  
62 and also investigated organic aerosol formation via aerosol mass spectrometry (Schroder et al.,  
63 2018). Finally, the LISTOS campaign in 2018 focused on measuring and modeling O<sub>3</sub> mixing  
64 ratios over the Sound to investigate the dynamics of O<sub>3</sub> formation linked to large metropolitan  
65 areas along the coast and associated downwind impacts (Zhang et al., 2020).

66         However, little is known about the molecular-level chemical composition of the gas-  
67 phase I/SVOCs and functionalized organic aerosol formed in the Northeastern U.S. This  
68 molecular-level speciation is key to understanding the physical/chemical properties of these  
69 compounds in the atmosphere and their chemical transformations, especially for classes of



70 compounds containing reduced and oxidized nitrogen functional groups, whose emissions,  
71 lifetime, and ultimate impacts are generally poorly understood. For example, nitrogen-containing  
72 compounds that serve as reservoir species for nitrogen oxides may increase the overall lifetime  
73 of nitrogen oxides in the atmosphere via renoxification mechanisms (e.g. the photolysis of  
74 particulate nitrates, which has been studied in the marine boundary layer (Ye et al., 2016)); some  
75 may act as light absorbing chromophores (e.g. the brown carbon studied from a methylglyoxal  
76 and ammonium sulfate system, which yielded mostly N-containing chromophores (Lin et al.,  
77 2015)); and some may have adverse, but uncertain, effects on human health (e.g. impacts on  
78 immune response to allergens (Ng et al., 2017)).

79         With the overall goal of examining the composition and contribution of nitrogen-  
80 containing organic compounds from mixed anthropogenic, biogenic, and marine sources, we  
81 collected measurements of organic gases and aerosols on the coast of the Long Island Sound in  
82 Guilford, Connecticut. We note that we used this site as a case study, but our observations of  
83 emissions and chemistry at this site are likely informative for other coastal urban and downwind  
84 regions due to the ubiquity of nitrogen-containing emissions from varied sources.

85         Samples were collected during the summer and winter, and analyzed via high resolution  
86 mass spectrometry to speciate the complex mixture of emissions and chemical transformation  
87 products. These samples were taken alongside several targeted pollutant measurements including  
88 O<sub>3</sub>, nitrogen oxides (NO<sub>x</sub>), particulate matter with a diameter of  $\leq 2.5 \mu\text{m}$  (PM<sub>2.5</sub>), and black  
89 carbon (BC), all to inform our chemically-speciated analyses, and to contribute to a longer-term  
90 characterization of this coastal area.

91         The objectives of this study were to: (1) investigate compositional trends and possible  
92 chemical pathways contributing to measured summer and winter functionalized organic aerosols



93 at this site; (2) examine the relative contributions of reduced and oxidized nitrogen groups to  
94 functionalized organic aerosol; and (3) use a novel sampling and liquid chromatography-based  
95 analytical approach to probe the molecular-level composition of functionalized gas-phase  
96 organic compounds and investigate possible nitrogen-containing gas-phase precursors to the  
97 observed reduced nitrogen-containing particles.

98

## 99 **2. Materials and Methods**

100 We collected measurements at the Yale Coastal Field Station (YCFS) in Guilford,  
101 Connecticut (41.26°N, 72.73°W) (Rogers et al., 2020). Inlets were positioned facing the Long  
102 Island Sound (i.e. South-Southeast) to capture onshore flow. The YCFS often received aged  
103 urban incoming air from East Coast metropolitan areas, similar to known common air parcel  
104 trajectories in the region (Figure S1). However, due to extensive mixing in the Northeast corridor  
105 and over the Long Island Sound, along with extended collection times for offline gas- and  
106 particle-phase samples, we also observed considerable biogenic and anthropogenic influence  
107 from other areas of the Northeastern U.S.

### 108 2.1. Offline Samples of Organic Particles and Gases Analyzed via Liquid and Gas

#### 109 Chromatography with Mass Spectrometry

110 We discuss three types of sampling and quadrupole time-of-flight mass spectrometry-  
111 based analyses here: particles collected on Teflon filters and analyzed using liquid  
112 chromatography with electrospray ionization, gases collected on packed adsorbent tubes and  
113 analyzed using gas chromatography with atmospheric pressure chemical ionization, and  
114 functionalized gases collected on cooled polyether ether ketone (PEEK) samplers and analyzed  
115 using liquid chromatography with electrospray ionization. Teflon filter and adsorbent tube



116 measurements were collected at the YCFS during the summer as part of the 2018 Long Island  
117 Sound Tropospheric Ozone Study (LISTOS), from July 9 to August 29, 2018. Additional filter  
118 and adsorbent tube samples were collected during the following winter from February 25 to  
119 March 5, 2019. Supplemental wintertime gas-phase samples on PEEK tubing were collected  
120 briefly from March 5-6 2020, prior to the COVID-19 shutdown.

121 For filter and adsorbent tube collection, we used a short inlet (0.9 m long, 5/8" OD  
122 stainless steel tubing, positioned 2.5 m above the ground) upstream of the sampler to allow the  
123 sampling media to be housed in an air-conditioned trailer. A stainless steel mesh screen (84  
124 mesh) was used at the opening of the inlet to limit particle size to  $\sim$ PM<sub>10</sub> and to prevent large  
125 particles from entering the sampler (Ditto et al., 2018). A custom filter and adsorbent tube  
126 housing was connected to the inlet to simultaneously collect particle- and gas-phase organic  
127 compounds, respectively (Sheu et al., 2018). The filter was positioned immediately upstream of  
128 the adsorbent tube to collect particles for analysis and to prevent particles from reaching the gas-  
129 phase sample. The housing was designed to minimize spacing between the filter and adsorbent  
130 tube to reduce gas-phase losses to upstream surfaces, and was built out of a modified passivated  
131 stainless steel filter holder and an aluminum block with sealed 6.34 mm (1/4") holes for  
132 adsorbent tubes (Sheu et al., 2018).

133 Teflon filters (47 mm, 2.0  $\mu$ m pores, Tisch Scientific) were used for particle-phase  
134 sampling. Filters were collected at 20 L/min for 8 hours, during the day (9:00am-5:00pm) and at  
135 night (9:00pm-5:00am). Samples were extracted in methanol and analyzed via liquid  
136 chromatography (LC) using an Agilent 1260 Infinity LC and an Agilent Poroshell 120 SB-Aq  
137 reverse phase column (2.1 x 50 mm, 2.7  $\mu$ m particle size). The LC was coupled to an  
138 electrospray ionization (ESI) source and a high-resolution mass spectrometer (Agilent 6550 Q-



139 TOF), and operated following previously described methods (Ditto et al., 2018, 2020). Filter  
140 extracts were run with MS (i.e. TOF-only, to identify molecular formulas) and MS/MS (i.e.  
141 tandem mass spectrometry, to identify functional groups) data acquisition, using both positive  
142 and negative mode electrospray ionization. These methods are hereafter referred to as “LC-ESI-  
143 MS” and “LC-ESI-MS/MS”, respectively. Acquisition and non-targeted analysis methods,  
144 including data QA/QC, are discussed in past work (Ditto et al., 2018, 2020). After stringent  
145 QA/QC for peak shape and accurate molecular formula determination, non-targeted compound  
146 identification from LC-ESI-MS examined an average of  $200\pm 56$  and  $167\pm 47$  compounds per  
147 sample analyzed in summer and winter, respectively, across 34 samples in summer and 15 in  
148 winter. For MS/MS, we used SIRIUS with CSI:FingerID for functional group identification with  
149 a subset of compounds from MS analysis (Dührkop et al., 2015, 2019), as detailed in past work  
150 (Ditto et al., 2020). We note that filter ion abundance data is presented as combined positive and  
151 negative ionization mode data, showing all compounds as having equal ionization efficiency.  
152 While exact ionization efficiency differences between compound types exist, their effects for  
153 multifunctional compounds present in a complex mixture are uncertain. Thus, similar to other  
154 studies and to our past work, we treat the intercomparison across compounds with equal  
155 ionization efficiencies (Ditto et al., 2018).

156 Gas-phase samples were collected on glass adsorbent tubes (6.35 mm OD, 88.9 mm long)  
157 packed with quartz wool, glass beads, Tenax TA, and Carbopack X (Sheu et al., 2018). Samples  
158 were collected at 200 mL/min for 2 hours, during the day (2:00-4:00pm) and at night (2:00-  
159 4:00am). Adsorbent tubes were analyzed using a GERSTEL TD3.5+ thermal desorption unit and  
160 an Agilent 7890B gas chromatograph (GC) with a DB5-MS UI column (30 m x 320  $\mu\text{m}$  x 0.25  
161  $\mu\text{m}$ ). The GC was coupled to an atmospheric pressure chemical ionization (APCI) source and the



162 same Q-TOF as above, operated with MS (i.e. TOF-only) data acquisition and positive ionization  
163 mode only. These methods are hereafter called “GC-APCI-MS” and acquisition and analysis  
164 methods are discussed in past work (Ditto et al., 2021; Khare et al., 2019). After QA/QC, this  
165 non-targeted analysis yielded an average of  $388\pm 201$  and  $612\pm 133$  compounds per sample in  
166 summer and winter, respectively, across 34 samples in summer and 14 samples in winter.

167 Finally, as a supplemental analysis to probe the composition of functionalized gases that  
168 were not GC amenable and thus not measured using the adsorbent tube and thermal desorption-  
169 gas chromatography techniques mentioned above, we used PEEK-based sample collectors and  
170 liquid chromatography to trap and speciate oxygen-, nitrogen-, and/or sulfur-containing gases  
171 without thermal desorption. This method was designed to target functionalized gases, which  
172 represent important precursors, intermediates, and by-products in the atmospheric processing of  
173 emitted organic compounds but are often challenging to speciate with traditional GC techniques  
174 due to their chemical functionality, reactivity, and/or thermal lability. Additionally, in many gas-  
175 phase measurement systems, primary emissions (i.e. hydrocarbons) can overwhelm the signal of  
176 more functionalized analytes, adding to the challenge of speciating these lower abundance  
177 compounds.

178 Thus, to probe the chemical composition of these functionalized gases, we used a  
179 sampling approach, desorption method, separation method, and ionization technique that  
180 leveraged their relatively lower volatility and higher polarity. This included adsorptive sampling  
181 onto cooled PEEK tubing followed by direct inline desorption into the LC mobile phase for LC-  
182 ESI-MS analysis. ESI was specifically chosen here because it is sensitive to functionalized  
183 compounds. Testing was performed in positive and negative ionization mode, but field samples  
184 were run in positive mode only. While further details and discussion can be found in Section S1



185 and Tables S1-3, briefly, PEEK tubing was cooled to 2°C and used as an adsorptive collector,  
186 with a Teflon filter positioned upstream of the PEEK tubing to remove particles. PEEK was  
187 selected due to its inert behavior, thus reducing the possibility for surface-analyte interactions  
188 that might inhibit effective inline solvent desorption and dissolution. PEEK is also compatible  
189 with the solvents used in the LC system, and is frequently used in LC instruments. Field samples  
190 were collected on cooled PEEK tubing during the subsequent winter (March 5-6, 2020), for 2  
191 hours each between 8:00am-2:00pm. For these 2 hour (~2.6 L) field samples, functionalized  
192 gases in a typical 100-250 g/mol molecular weight range were resolvable at ~25-60 ppt in the  
193 atmosphere, based on instrument detection limits (Ditto et al., 2018). For analysis, each PEEK  
194 collector was installed in the LC system flow path, and analytes were directly desorbed using the  
195 LC mobile phase solvents then trapped and focused on the LC column for 20 minutes, before  
196 being analyzed using the same LC-ESI-MS system in positive ionization mode (Figure 1). This  
197 inline mobile phase desorption step gently mobilized potentially fragile analytes from the PEEK  
198 collector and trapped and focused them on the LC column prior to chromatographic separation  
199 and mass spectral analysis. Additionally, this preconcentration step allows for the detection and  
200 characterization of lower concentration species.

201 We note that there are other existing approaches for offline collection of highly-  
202 functionalized organic gases and particles that are compatible with LC analysis such as spray  
203 chambers, particle into liquid samplers, coated denuders, PUF sampling, and more. This PEEK  
204 sampling method with inline desorption into the LC mobile phase was pursued to reduce sample  
205 preparation steps and thus possibilities for losses (e.g. during solvent extraction or evaporative  
206 preconcentration), as well as for its direct similarity to the filter-based particle-phase LC-ESI-MS  
207 analysis.



208 We also note that for all LC analyses, it is possible that some functional groups of interest  
209 (e.g. organonitrates) may have undergone hydrolysis in the LC mobile phase, which was  
210 primarily water at the beginning of the LC solvent gradient. If so, some of the observed  
211 compounds could be byproducts of other functionalized species, though this would require  
212 hydrolysis to occur on the order of a few minutes. While we did not observe any of our nitrogen-  
213 containing test standards to hydrolyze over these timescales, standards were not available to  
214 reflect every functional group observed in these datasets.

## 215 2.2. Supporting Measurements

216 O<sub>3</sub>, NO<sub>x</sub>, PM<sub>2.5</sub>, and BC concentrations were recorded concurrently during both summer  
217 and winter sampling periods. O<sub>3</sub> was measured with a 2B Tech Model 202 Ozone Monitor, NO<sub>x</sub>  
218 with a Thermo Scientific Model 42i-TL Analyzer, PM<sub>2.5</sub> with a MetOne BAM-1020 instrument,  
219 and BC with a Magee Scientific AE33 Aethalometer. O<sub>3</sub> and NO<sub>x</sub> inlets were constructed of FEP  
220 tubing (1/4" OD), with a Teflon filter housed in a PFA filter holder upstream to remove particles.  
221 The PM<sub>2.5</sub> inlet was made of stainless steel tubing (1 1/4" OD) and the BC inlet was made of  
222 copper tubing (3/8" OD). Both particle inlets were outfitted with a PM<sub>2.5</sub> cyclone to limit particle  
223 size to 2.5 μm and below.

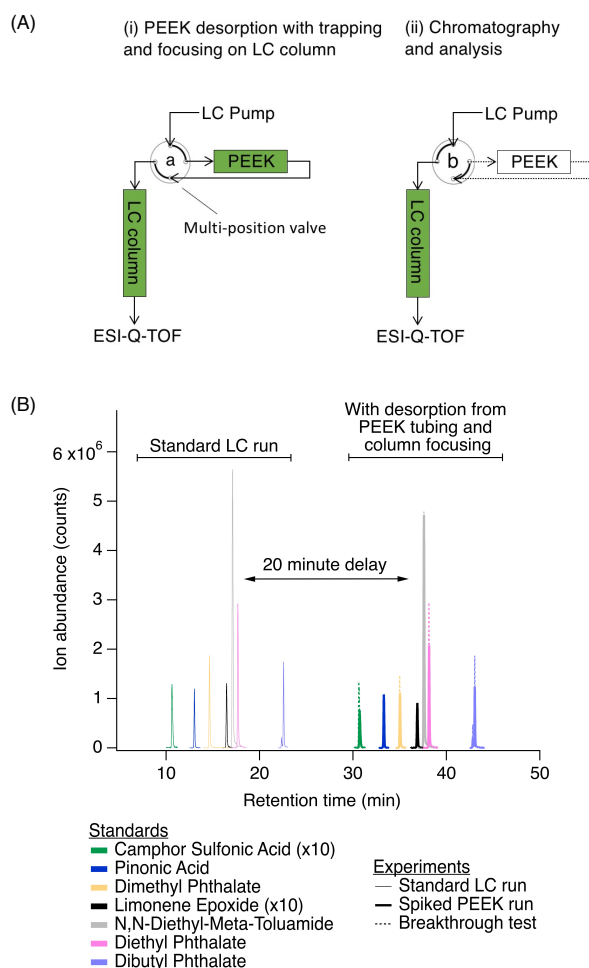
224 All inlets were mounted 3 m above the ground. Instrument flow rates were calibrated  
225 with an external mass flow controller. O<sub>3</sub> and NO<sub>x</sub> monitors were zeroed with laboratory-  
226 generated zero air. The O<sub>3</sub> monitor was calibrated against Connecticut Department of Energy and  
227 Environmental Protection instrumentation and further confirmed with an O<sub>3</sub> generator in the lab.  
228 The NO<sub>x</sub> monitor was calibrated using a NO standard (AirGas, 2 ppm NO in nitrogen, ± 5%)  
229 diluted to 25 ppb with laboratory-generated nitrogen gas. The BC instrument was programmed to  
230 conduct an automatic performance check using particle-free air and the PM<sub>2.5</sub> instrument was



231 zeroed following MetOne protocols with particle-free air. O<sub>3</sub> and NO<sub>x</sub> data were collected at 1-  
232 second intervals, BC data were collected at 1-minute intervals, and PM<sub>2.5</sub> data were collected at  
233 1-hour intervals. BC data were saved directly from the instrument, while O<sub>3</sub>, NO<sub>x</sub>, and PM<sub>2.5</sub>  
234 data were recorded with a LabJack T7 datalogger and custom LabView code. In addition, hourly  
235 weather data (temperature, relative humidity, wind speed, wind direction) were collected with a  
236 WeatherHawk weather station on top of the 3 m tower.

237       During the summer, we also collected a small number of size-resolved particle samples  
238 on quartz filters using an eight-stage cascade impactor (Thermo Scientific). Quartz filters were  
239 extracted and analyzed following the same procedure as the Teflon filters discussed above, with  
240 the addition of a syringe filtration step to remove insoluble fibers. The cascade impactor was  
241 positioned on the roof of the trailer and pulled 28.3 L/min through the inlet for periods of 8 hours  
242 during the day and at night (same timing as above) or for 24-hour periods.

243       Finally, we computed 48-hour backward trajectories for every hour during each offline  
244 sample collection period with the HYSPLIT Backward Trajectory Model (accessed online at  
245 <https://www.ready.noaa.gov/HYSPLIT.php>), using GDAS1.0 meteorological data, the field site's  
246 coordinates as each trajectory's end point, and a final trajectory height of 50 m above the ground.



247 **Figure 1.** (A) Simplified analytical system setup for functionalized gas-phase compounds,  
248 showing (i) desorption from the PEEK collector and trapping on the LC column in order to focus  
249 analytes prior to chromatographic separation, and (ii) subsequent chromatographic separation  
250 and analysis. Green shading indicates active solvent flow through PEEK collector and/or LC  
251 column. A multi-position valve was switched from position “a” (panel (i)) to position “b” (panel  
252 (ii)) to remove the PEEK collector from the flow path for chromatography and analysis. Table S1  
253 describes the flow rates and solvents used in each of these steps. (B) Comparison of select peaks  
254 from a typical LC run (solid traces from 10-23 min) to that from a PEEK collector spiked with a  
255 standard (bold traces from 30-43 min) demonstrates desorption, trapping/focusing, and similar  
256 chromatography. Comparable results from a 2-hour breakthrough test at 2°C with 22 mL/min air  
257 flow are also shown (overlaid dotted traces from 30-43 min). Spiked PEEK and breakthrough  
258 tests were performed to validate this sampling and analysis methods, and are discussed further in  
259 Section S1. Test analytes were used across a range of functionality, with examples shown here  
260 and the full list in Table S2.



261 **3. Results and Discussion**

262 3.1. Characteristics of the Urban Regional Site

263 Backward trajectories for summertime and wintertime samples showed a strong urban  
264 influence. Summertime trajectories ranged from the northwest, west, and especially the  
265 southwest (i.e. New York City and other coastal metropolitan areas, similar to well-established  
266 and expected air flow patterns near the Long Island Sound). In contrast, trajectories were almost  
267 exclusively from the northwest in the winter (Figure S1). These air parcels brought a range of  
268 compounds from a mixture of anthropogenic, biogenic, and marine sources to the site, all with  
269 differences in gas- and particle-phase source profiles. However, due to the varied backward  
270 trajectories, dynamic variations in wind direction over the long duration filter samples (Figure  
271 S2), and a high degree of mixing over the Sound, our 8-hour samples are representative of mixed  
272 regional conditions in summer and winter, and are thus discussed in this context. Further detailed  
273 site characterization can be found in Section S2 and Figures S1-S3.

274 3.2. Seasonal Comparisons of Functionalized Organic Aerosols

275 3.2.1. Summertime composition and the influence of photochemistry and  $NO_x$

276 During this period of active photochemistry, the observed distribution of particle-phase  
277 compounds in summertime samples spanned across the intermediate volatility (IVOC) to  
278 ultralow volatility organic compound (ULVOC) range, with a predominance of semivolatile  
279 (SVOC), low volatility (LVOC), and extremely low volatility organic compounds (ELVOC)  
280 (Figure 2A). These compounds existed across a range of functionality. Due to elevated  
281 summertime  $O_3$  mixing ratios at the site (shown in Figure S2, 8-hour maximum mixing ratio in  
282 summer:  $57 \pm 20$  ppb, vs. winter:  $46 \pm 5$  ppb,  $p < 0.05$ , including day and night sampling  
283 periods),  $O_3$  may have influenced the photochemical processing of emitted volatile species,



284 especially unsaturated biogenic VOCs which readily undergo ozonolysis due to their chemical  
285 structure. However, we did not observe a correlation between 8-hour maximum (or 8-hour  
286 average) O<sub>3</sub> mixing ratios with average particle-phase volatility, carbon number, or O/C (nor did  
287 we observe such relationships for gas-phase organic compounds). There were, however, weak  
288 relationships between NO<sub>x</sub> mixing ratios and each of these particle-phase characteristics in the  
289 summer. While average NO<sub>x</sub> mixing ratios were slightly lower during the summer (as shown in  
290 Figure S2,  $2.3 \pm 1.5$  ppb in summer vs.  $3.7 \pm 2.7$  ppb in winter,  $p < 0.05$ ), NO<sub>x</sub> mixing ratios  
291 trended weakly with particle-phase O/C ( $r \sim 0.45$ ), volatility (as saturation mass concentration,  
292  $\log(C_0)$ ,  $r \sim 0.49$ ), and inversely with carbon number ( $r \sim -0.56$ ) in summer.

293         While our correlations and conclusions are somewhat limited by the 8-hour filter  
294 sampling duration and the resulting highly regionally-mixed samples, one possible hypothesis is  
295 that the presence of NO<sub>x</sub> could have promoted more fragmentation reactions in the gas-phase  
296 (Loza et al., 2014) that decreased average carbon number, and correspondingly increased  
297 volatility and O/C. In fact, we observed highly oxidized C<sub>3</sub>-C<sub>6</sub> compounds in the gas-phase (from  
298 adsorbent tube measurements with GC-APCI (Section S2)) that were possibly products of these  
299 fragmentation reactions of larger compounds. These trends of NO<sub>x</sub> mixing ratios with O/C,  
300 volatility, and carbon number were not apparent for the observed complex mixture of gas-phase  
301 organic compounds. However, these highly oxidized gases may not have persisted in the gas-  
302 phase and could have been taken up by the condensed/aqueous phase due to their water  
303 solubility, where they would have instead contributed to the observed trends of NO<sub>x</sub> with carbon  
304 number, volatility, and O/C in the particle-phase. We note that if there was significant uptake of  
305 gas-phase NO<sub>z</sub> to the particle-phase, this may have in part contributed to the particle-phase



306 correlations with NO<sub>x</sub> given that the chemiluminescence NO<sub>x</sub> analyzer used in this study is  
307 known to also respond to gas-phase NO<sub>z</sub> (Dunlea et al., 2007).

308 Additionally, NO<sub>x</sub> could have been involved in heterogeneous chemistry, promoting  
309 oxidation and/or nitrogen addition reactions, such as interaction with NO<sub>3</sub><sup>\*</sup> to yield organonitrates  
310 (Lim et al., 2016), formation and interaction with HONO to yield nitrophenols (Vidović et al.,  
311 2018), or other pathways.

### 312 3.2.2. Comparison to wintertime composition and the role of aqueous-phase chemistry

313 In the winter, these same relationships between NO<sub>x</sub> and particle-phase characteristics  
314 were not observed. This is possibly due to the decreased role of photochemistry in the winter and  
315 the increased role of other competing physical and chemical processes, such as aqueous-phase  
316 chemistry. The observed chemical composition of the particle-phase in the winter was indeed  
317 indicative of increased aqueous-phase processing, with a shifted compound distribution that  
318 included lower molecular weight and higher volatility particle-phase species compared to  
319 summer (shown by saturation mass concentration in Figure 2A-B). This is consistent with  
320 another past study that suggested that aged fog-water samples contained organic compounds with  
321 smaller carbon backbone structures than aged non-aqueous particles, and linked this difference to  
322 aqueous-phase fragmentation reactions, the uptake of smaller water-soluble gases to the aqueous-  
323 phase, and/or less oligomerization (Brege et al., 2018). In contrast, there was a larger proportion  
324 of LVOCs, ELVOCs, and ULVOCs in summer, which decreased the average summertime  
325 volatility of the functionalized organic aerosol components. This was likely driven by increased  
326 photochemical processing in summer, leading to lower saturation mass concentrations (summer:  
327  $\log(C_0) = -4.1 \pm 5.0 \mu\text{g}/\text{m}^3$ , vs. winter:  $\log(C_0) = -1.8 \pm 4.8 \mu\text{g}/\text{m}^3$ ,  $p < 0.05$ ) and higher O/C  
328 (summer: O/C =  $0.5 \pm 0.4$  vs. winter: O/C =  $0.4 \pm 0.4$ ,  $p < 0.05$ ). To assess the potential



329 contribution of aqueous-phase chemistry, we also estimated aerosol liquid water concentrations  
330 based on available data in Section S2.1.

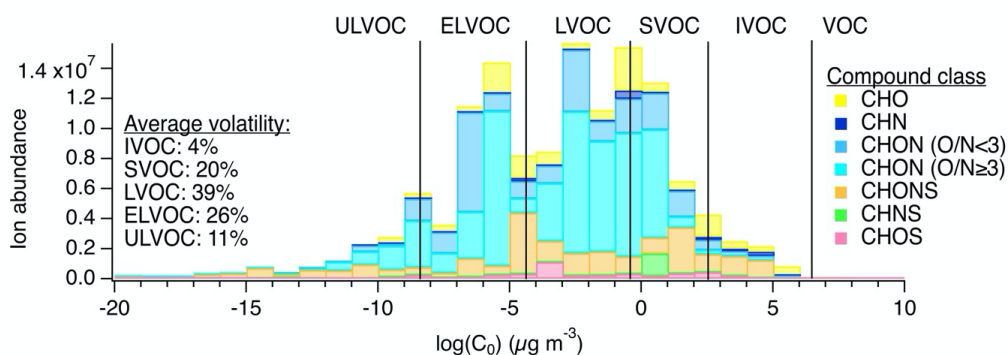
331 Furthermore, from MS/MS analysis, we observed functional groups that were possible  
332 indicators of aqueous-phase processing, including the presence of nitrophenols during the winter,  
333 which may have formed via dark aqueous-phase reactions with HONO (Vidović et al., 2018),  
334 and relatively low contributions from carbonyls across seasons, possibly linked to carbonyl  
335 hydrolysis (Ditto et al., 2020). Based on laboratory studies, the presence of azole functional  
336 groups and other heterocyclic nitrogen species could also indicate aqueous phase processing, and  
337 may be formed from small carbonyl precursors such as glyoxal (DeHaan et al., 2009; Grace et  
338 al., 2019) and biacetyl (Grace et al., 2020) reacting with atmospheric ammonia or small amines.  
339 Many of the N-only containing azoles observed here had similar substructures to those formed in  
340 the aqueous-phase reactions of small carbonyls with ammonia/amines (DeHaan et al., 2009;  
341 Grace et al., 2019). In addition, as discussed above, we observed many small gas-phase C<sub>3</sub>-C<sub>6</sub>  
342 compounds at the site in the summer, which likely included multifunctional isoprene oxidation  
343 products (e.g. glycoaldehyde, hydroxyacetone, and isomers); these potential precursors could  
344 have reacted with atmospheric ammonia or species containing amino groups to form the  
345 observed azole-containing reaction products. We observed more azoles during the summer (Ditto  
346 et al., 2020), perhaps due to the increased prevalence of the C<sub>3</sub>-C<sub>6</sub> precursors and overall  
347 prominence of aerosol liquid water.

348 Lastly, the role of aqueous-phase chemistry in the region is further supported by prior  
349 summertime observations at Brookhaven National Laboratory (on the opposite side of the Long  
350 Island Sound), which examined a low-volatility oxygenated organic aerosol factor in the source  
351 apportionment of aerosol mass spectrometry measurements, and showed a strong contribution

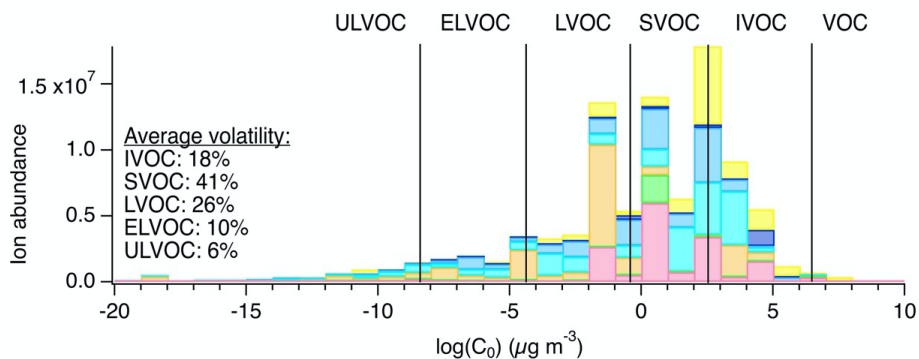


352 from carboxylic acids and other ELVOCs that were attributed to aqueous-phase processing  
353 (Zhou et al., 2016).

(A) Particle-phase summer volatility distribution (LC-ESI-MS)



(B) Particle-phase winter volatility distribution (LC-ESI-MS)



354 **Figure 2.** Chemical composition of particle-phase organic compound mixtures at the YCFS from  
355 LC-ESI-MS measurements. (A) and (B) show particle-phase volatility distributions by  
356 compound class in the summer (N=34) and winter (N=15), respectively. Compound volatility  
357 was estimated and grouped following approaches in the literature (Li et al., 2016; Schervish and  
358 Donahue, 2020). For direct comparison, volatility bins were defined for the same reference  
359 temperature in (A) and (B) (i.e. 300 K, the average summertime sampling period temperature),  
360 though wintertime saturation mass concentrations for the observed compounds would shift  
361 approximately 2 orders of magnitude lower due to lower temperatures (i.e. 270K). Thus, in the  
362 winter, a larger fraction of I/SVOCs would have partitioned to the particle phase, though this  
363 effect was likely more pronounced for SVOCs than IVOCs (see Table S4).



364 3.2.3. Comparison to other sites

365           The distribution of compound classes observed at the YCFS was significantly different  
366 from observations at a range of field sites discussed in past studies (Figure 3), including a remote  
367 forested site (i.e. the PROPHET site in Northern Michigan), an urban inland site (i.e. near  
368 downtown Atlanta) across two seasons, and in New York City (Ditto et al., 2018, 2019). While a  
369 detailed site-to-site comparison is outside the scope of this work, the proximity of the YCFS to  
370 the ocean and thus the impact of marine emissions and over-water chemistry likely contributed to  
371 the differences between the YCFS and inland locations.

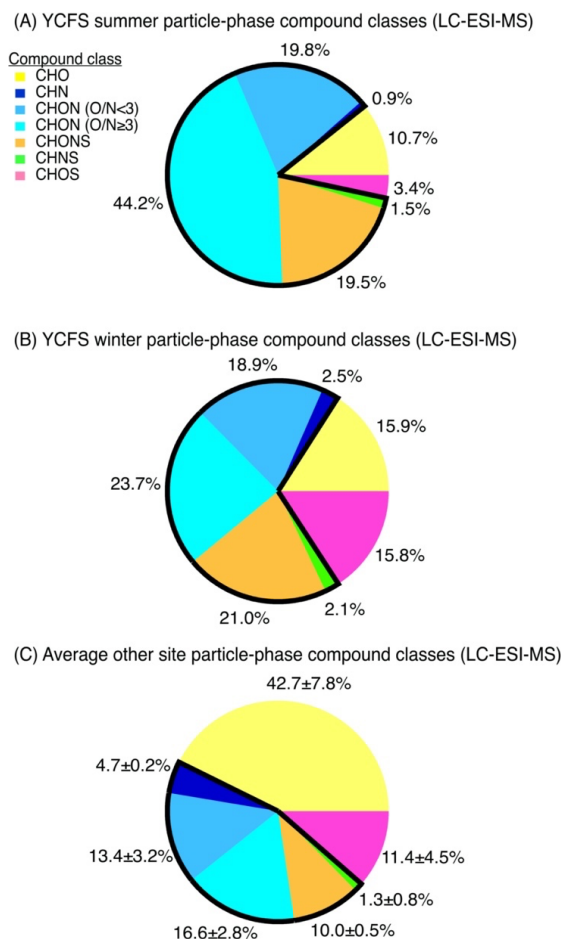
372           In particular, at the YCFS, we observed notably smaller relative contributions from  
373 compounds containing carbon, hydrogen, and oxygen (i.e. CHO, 11-16% of observed  
374 functionalized compounds here vs. 34-50% at other sites), and the contributions from nitrogen-  
375 containing particle-phase compounds at the YCFS were in stark contrast to other sites. Here,  
376 85% of compounds in summer and 68% of compounds in winter contained at least one nitrogen  
377 atom, compared to 38-51% at the other previously studied sites (Figure 3). These nitrogen-  
378 containing species were comprised of compounds with various reduced and oxidized nitrogen-  
379 containing functional groups with varying oxygen-to-nitrogen ratios (O/N), which are broadly  
380 classified and discussed below as compounds containing carbon, hydrogen, and nitrogen (i.e.  
381 CHN), and compounds containing carbon, hydrogen, oxygen, and nitrogen (i.e. CHON (O/N  
382 ratio < 3), and CHON (O/N ratio ≥ 3)). There were notably greater contributions at the site from  
383 nitrogen-containing compounds that also contained at least one oxygen atom, including CHON  
384 compounds with O/N < 3 (19-20% here vs. 10-15% at other sites), CHON compounds with O/N  
385 ≥ 3 (24-44% here vs. 14-19% at other sites), as well as compounds containing oxygen, nitrogen,



386 and sulfur (i.e. CHONS, 20-21% here vs. 9-10% at other sites) (Ditto et al., 2018). See Section  
387 S3 and Figure S4 for discussion of additional compound classes.

388 We note that while these were PM<sub>10</sub> measurements, the observations of high nitrogen  
389 content were not biased by the inclusion of larger, possibly primary particles. Quartz filter  
390 samples collected with a cascade impactor at the site during the summer and analyzed with the  
391 same LC-ESI-MS methods did not show any statistically significant differences between any of  
392 these nitrogen-containing compound classes as a function of particle size across particles ranging  
393 from 0.4 to 10 μm. This is consistent with past studies which have demonstrated that amines, as  
394 an example of reduced nitrogen, are ubiquitous in size-resolved aerosol samples in urban and  
395 rural locations (VandenBoer et al., 2011).

396 The prevalence of nitrogen-containing species at the YCFS is consistent with the study at  
397 Brookhaven National Laboratory discussed above, where a dedicated nitrogen-enriched aerosol  
398 mass spectrometry factor was identified, and contained prevalent signal from aliphatic amines  
399 and amides. However, in the Brookhaven study, the nitrogen-enriched factor was associated with  
400 industrial amine emissions that were enhanced during periods of south/southwestern backward  
401 trajectory influence, and that had correlations with tracers linked to industrial processes. In our  
402 study, there was no correlation between backward trajectory direction and the contribution of  
403 nitrogen-containing species. Also, wintertime air parcels arrived predominantly from directions  
404 other than south/southwest, suggesting that the nitrogen-containing species observed in our study  
405 were the result of mixed anthropogenic, biogenic, and marine precursors and their transformation  
406 products.



407 **Figure 3.** Enhancements in nitrogen-containing particle-phase compounds compared to other  
408 sites, from LC-ESI-MS measurements. Particle-phase compound class distributions in the  
409 summer (A) and winter (B) at the YCFS, weighted by compound abundance, in contrast with the  
410 average compound class distribution from previously studied forested, urban inland, and urban  
411 coastal sites (C). Nitrogen-containing compound class contributions are outlined in black.

### 412 3.3. Speciating Particle-Phase Multifunctional Nitrogen-Containing Compounds

414 The observed particle-phase species were highly functionalized, often multi-functional,  
415 and contained combinations of oxygen, nitrogen, and/or sulfur heteroatoms. Here, we discuss the  
416 functional groups present, broken up by the nitrogen-containing compound classes shown in  
417 Figures 2-3, with additional discussion of other relevant compound classes in Section S3.



418 3.3.1. CHN compounds

419 While nitrogen-containing compounds in general were very prominent at the site (Figure  
420 3A-B), CHN compounds were relatively less abundant in these samples of functionalized  
421 organic aerosol. Particle-phase CHN compounds represented just 1% and 3% of observed  
422 functionalized organic aerosol abundance in summer and winter, respectively, which was similar  
423 to observations at other ambient sites (~5% CHN) (Ditto et al., 2018).

424 In the summertime LC-ESI-MS/MS measurements, CHN particle-phase compounds were  
425 comprised primarily of amines (72% of CHN species contained an amine group) and nitriles  
426 (28% of CHN species contained a nitrile group), as shown in Figure 4. In the winter, these  
427 compounds were nearly exclusively amines (present in 99% of CHN species). Amines have  
428 many primary land-based sources (e.g. biogenic emissions (Kieloaho et al., 2013), agricultural  
429 activity (Ge et al., 2011), emissions from decomposing organic matter (Ge et al., 2011;  
430 Sintermann and Neftel, 2015), biomass burning (Ge et al., 2011), emissions from port activity  
431 (Gaston et al., 2013), chemical products (Khare and Gentner, 2018), and vehicle exhaust  
432 (Sodeman et al., 2005)), but their presence on the coast could also indicate marine contributions.  
433 Amines have been detected both in bulk ocean water, the surface microlayer, and in sea spray  
434 aerosol, and their emissions and chemical transformations in the marine environment have been  
435 the topic of many recent studies (e.g. Brean et al., 2021; Dall'Osto et al., 2019; Decesari et al.,  
436 2020; Di Lorenzo et al., 2018; van Pinxteren et al., 2012, 2019; Quinn et al., 2015; Wu et al.,  
437 2020).

438 Recent studies have also evaluated amine phase partitioning or formation in cloud/fog  
439 water (e.g. Chen et al., 2018; Youn et al., 2015), as well as condensed-phase or aqueous-phase  
440 pathways that may transform emitted amines (e.g. Ge et al., 2016; Lim et al., 2019; Tao et al.,



2021). Interestingly, the observed amines at this site, as well as other reduced nitrogen groups like nitriles, imines, and enamines, were not present exclusively in CHN species and thus were a mix of both direct emissions and chemically processed compounds. Reduced nitrogen groups were often paired with hydroxyl groups, carboxylic acids, carbonyls, ethers, and esters as part of nitrogen and oxygen containing compounds with a range of O/N ratios. As such, we discuss CHON species as a function of O/N ratio to focus on differences between less-oxygenated ( $O/N < 3$ ) and more-oxygenated ( $O/N \geq 3$ , e.g. organonitrates) species, using a ratio of 3 to distinguish between the two as informed by the O/N ratio of the organonitrate functional group.

### 3.3.2. CHON ( $O/N < 3$ ) compounds

CHON ( $O/N < 3$ ) compounds were notably more important at this site than other sites, representing 20% and 19% of observed functionalized organic aerosol abundance in summer and winter, respectively (Figure 3A-B), compared to ~13% at other sites (from predominantly summer measurements). These CHON compounds included some functional groups that contained both oxygen and nitrogen, such as amide groups (12% of this compound class's nitrogen content in summer, vs. 1% in winter, Figure 4) and nitro groups (15% of this nitrogen content in summer, vs. 6% in winter, Figure 4). However, most CHON ( $O/N < 3$ ) compounds were comprised of a combination of nitrogen- *or* oxygen-containing groups, rather than a functional group containing both nitrogen and oxygen. This included large contributions from hydroxyls and ethers across both seasons, as well as important contributions from amines, isocyanates, and heterocyclic nitrogen (Ditto et al., 2020). The presence of these functional groups in the winter could be indicative of wood burning emissions in the region, which has been observed in the wintertime in past ambient sampling in the Northeast U.S. (Sullivan et al., 2019). Isocyanates contributed notably to this compound class during the winter, which could similarly



464 be linked to burning wood, other biomass, building materials (Leslie et al., 2019; Priestley et al.,  
465 2018; Roberts et al., 2014), or could be photochemically produced via the oxidation of amines  
466 and amides (Borduas et al., 2015; Leslie et al., 2019). Importantly, levoglucosan, a common  
467 biomass burning tracer, was observed across nearly all daytime and nighttime winter particle-  
468 phase samples (verified with an authentic standard), supporting the influence of biomass burning  
469 compounds at the site. Together, the overall high prevalence of reduced nitrogen at this site  
470 could be influenced by the mixing of aged biomass burning plumes with marine air, which is  
471 consistent with past observations of very high alkylamine concentrations in biomass burning  
472 particles that mixed with marine air prior to sampling (Di Lorenzo et al., 2018).

### 473 3.3.3. CHON ( $O/N \geq 3$ ) compounds

474 CHON ( $O/N \geq 3$ ) compounds were the dominant compound class in the observed  
475 summertime distribution and played an important role in the wintertime distribution as well,  
476 comprising 44% of observed functionalized organic aerosol abundance in summer vs. 24% in  
477 winter (Figure 3A-B). These contributions were far greater than the contributions of CHON ( $O/N$   
478  $\geq 3$ ) species at other sites, which typically ranged from 14-19% (predominantly from  
479 summertime measurement, Figure 3C).

480 Similar to CHON ( $O/N < 3$ ), we observed some CHON ( $O/N \geq 3$ ) compounds with  
481 functional groups containing 3 oxygen atoms and 1 nitrogen atom, e.g. nitrophenols and  
482 organonitrates (Figure 4), but also contributions from nitrogen-only functional groups paired  
483 with oxygen-containing groups. Notably, in the summer, there were important contributions from  
484 amines (47% of this compound class's nitrogen content), imines (19%), organonitrates (10%),  
485 and azoles (16%) (Figure 4). In contrast, in the winter, nitrogen content in the CHON ( $O/N \geq 3$ )



486 compound class was dominated by I/SVOC nitrophenols, comprising 64% of the CHON ( $O/N \geq$   
487 3) ion abundance.

488  $NO_x$  mixing ratios were typically low in both summer and winter ( $2.3 \pm 1.5$  ppb in  
489 summer vs.  $3.7 \pm 2.7$  ppb in winter), but were slightly higher during winter. In the winter, CHON  
490 ( $O/N \geq 3$ ) compounds showed a weak positive relationship with  $NO_x$  mixing ratios ( $r \sim 0.58$ ) and  
491 a stronger correlation with NO mixing ratios ( $r \sim 0.81$ ). This relationship between CHON ( $O/N \geq$   
492 3) and NO (and  $NO_x$ ) suggests that many of these oxidized nitrogen species were products of  
493  $NO_x$ -related chemistry (i.e.  $NO_z$  compounds). The enhancements in nitrophenols serves as one  
494 example of this, as NO mixing ratios also correlated with the contribution of nitrophenols in the  
495 winter ( $r \sim 0.69$ ).

496 In past work, we discussed nitrophenol nighttime enhancements during winter, and noted  
497 their reported aqueous formation pathways mentioned in prior laboratory studies (Ditto et al.,  
498 2020). Here, we demonstrate that nitrophenols were important contributors to the CHON ( $O/N \geq$   
499 3) compound class, and highlight their role as examples of  $NO_z$  due to their possible formation  
500 via dark aqueous-phase nitration pathways of oxygenated aromatics with ambient nitrous acid  
501 (HONO) (Vidović et al., 2018). While nitrophenols may have other sources (e.g. diesel exhaust),  
502 our observations of a clear nighttime enhancement during the winter suggest that these functional  
503 groups were most likely formed by secondary chemistry related to  $NO_x$  oxidation, as this field  
504 site was removed from major roadways. Our wintertime observations suggest that HONO could  
505 have been derived from local wood burning, and could have reacted away as the smoke plume  
506 aged to form stable products like nitrophenols, similar to HONO transformation chemistry into  
507 other forms of oxidized nitrogen (e.g. particulate nitrates, PANs, organic nitrates) that has  
508 recently been observed in wildfire smoke (Juncosa Calahorrano et al., 2021).



509 Furthermore, the correlation between NO and CHON ( $O/N \geq 3$ ) could also be influenced  
510 by the daytime formation of organonitrates via reaction with  $OH^\bullet$  and NO (i.e.  $RO_2^\bullet + NO$ )  
511 (Liebmann et al., 2019; Ng et al., 2017; Perring et al., 2013; Takeuchi and Ng, 2018), though  
512 organonitrates contributed to a smaller fraction of CHON ( $O/N \geq 3$ ) species (i.e. 10% of this  
513 compound class's nitrogen content across seasons).

#### 514 3.3.4. Overall contributions of reduced and oxidized nitrogen groups

515 In the summer and winter, contributions from reduced nitrogen groups (e.g. groups  
516 shown in black/grey in Figure 4) rivaled that of oxidized nitrogen groups in CHON compounds  
517 across a range of O/N ratios. In the summer, reduced nitrogen groups contributed to 50% of all  
518 detected CHON ( $O/N < 3$ ) compounds by ion abundance, while in the winter they contributed  
519 47% (Figure 4). For CHON compounds with  $O/N \geq 3$ , reduced nitrogen groups contributed to  
520 68% of compound ion abundance in the summer, while in the winter they contributed just 13%.  
521 Interestingly, 90% of the dominant reduced nitrogen functional groups observed (amines and  
522 imines) were present in acyclic rather than cyclic structures, which may have been the result of  
523 either direct emissions or formation via reactions with ammonia or other small amines.

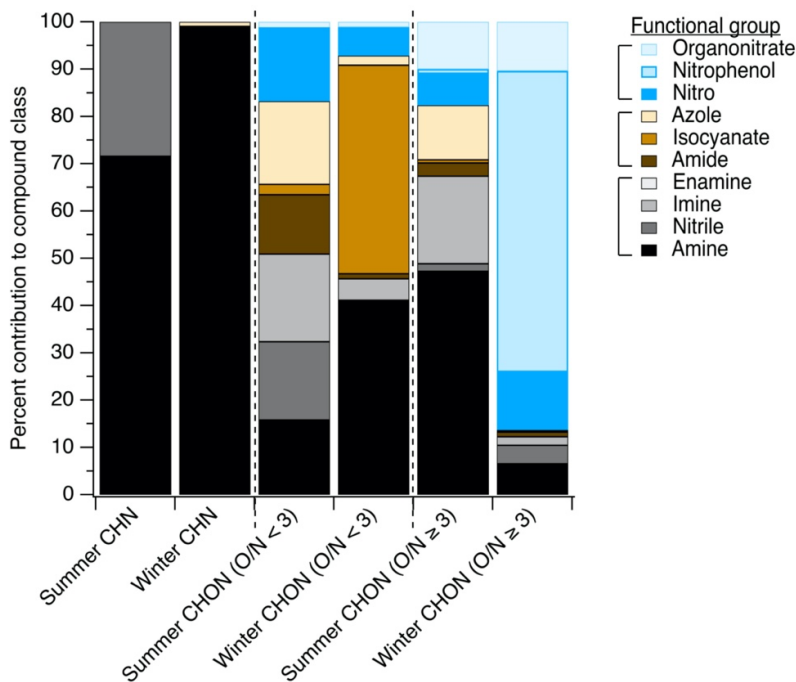
524 In contrast, possible  $NO_x$  products (e.g. groups shown in blue in Figure 4) were present in  
525 18% and 7% of CHON ( $O/N < 3$ ) compounds in the summer and winter, respectively. For  
526 CHON ( $O/N \geq 3$ ) compounds, they were present in 18% and 86% in the summer and winter,  
527 respectively, with the latter wintertime increase in oxidized N-groups largely driven by the  
528 presence of nitrophenols at night (Ditto et al., 2020). The remaining fraction of nitrogen-  
529 containing groups also contained oxygen, but with a reduced nitrogen atom (e.g. amide,  
530 isocyanate, nitrogen/oxygen-containing azole, shown in brown in Figure 4). We note that



531 CHONS compounds also represented a sizable fraction of observed organic nitrogen (Figure 3),  
532 and contained a mix of reduced and oxidized functional groups (Section S3 and Figure S4).

533 The importance of reduced nitrogen functional groups in CHON compounds highlights  
534 that not all oxygen- and nitrogen-containing species in the CHON ( $O/N \geq 3$ ) compound class  
535 were  $NO_z$ , despite their apparent molecular formulas and the observed correlation observed  
536 between CHON ( $O/N \geq 3$ ) species with NO and  $NO_x$  mixing ratios. For instance, many of the  
537 observed reduced nitrogen-containing functional groups co-occurred with several oxygen-  
538 containing groups like hydroxyls, carboxylic acids, esters, ethers, and carbonyls, and thus had  
539 molecular formulas with  $O/N \geq 3$ , which could incorrectly be assumed to be an organonitrate or  
540 similar structure based on molecular formula alone.

541 We note that the relative distribution of reduced and oxidized nitrogen-containing groups  
542 shown here is subject to sampling and ionization conditions. While the electrospray ionization  
543 source used for the particle-phase analysis discussed here effectively ionized these nitrogen-  
544 containing groups, their relative sensitivity may differ because many of these functional groups  
545 were present in multifunctional compounds whose other features may also contribute to  
546 ionization behavior. Also, other aspects of the sample collection and extraction process could  
547 cause variability in observed signal (e.g. PM size cut, organonitrate stability over long duration  
548 samples). Thus, we emphasize that the observed relative abundances here are valuable because  
549 they suggest that fully reduced nitrogen-containing groups are important contributors to  
550 multifunctional CHON species, but their exact mass contributions remain uncertain.



551 **Figure 4.** The distribution of functional groups in particle-phase nitrogen-containing compounds  
552 measured via LC-ESI-MS/MS. The breakdown of CHN, CHON ( $O/N < 3$ ), and CHON ( $O/N \geq$   
553  $3$ ) compounds is shown as a function of contributions of each functional group to ion abundance,  
554 with possible  $NO_z$  species shown in blue shades, fully-reduced nitrogen-containing groups  
555 shown in black/grey shades, and groups containing both oxygen and nitrogen where the nitrogen  
556 atom itself is not oxidized shown in brown shades.

### 557 3.4. Probing Possible Nitrogen-Containing Gas-Phase Precursors to Observed Nitrogen- 558 Containing Particles with Adsorptive Sampling and LC-ESI-MS

559 The particle-phase volatility distribution in the winter consisted of 18% IVOCs and 41%  
560 SVOCs (Figure 2B). Of the observed compounds in winter, 68% contained nitrogen; these likely  
561 included contributions from functionalized gas-phase precursors and likely were influenced by  
562 the active multiphase partitioning of these precursors, and their gas- or particle-phase reaction  
563 products, with changes in organic aerosol loading, atmospheric liquid water concentrations, and



564 temperature (Donahue et al., 2011; Ervens et al., 2011). This emphasizes the need to measure a  
565 broader range of these functionalized gas-phase compounds, which have known limitations with  
566 GC transmission, but represent uncertain and important-to-measure SOA precursors.

567         However, despite evidence of substantial contributions from particle-phase I/SVOCs with  
568 diverse nitrogen-containing functionalities that could dynamically partition between phases  
569 (Figure 2A-B), the observed compound class distribution from gas-phase adsorbent tube  
570 measurements analyzed via GC-APCI-MS was dominated by hydrocarbons (i.e. CH, 24% of  
571 detected ion abundance in summer vs. 18% in winter) and oxygenates (i.e. CHO, 66% in summer  
572 vs. 69% in winter) (Figure S5). These gas-phase species appeared to be lightly functionalized  
573 oxygenates (average O/C:  $0.12 \pm 0.13$ ), showing minimal contributions from nitrogen (or sulfur)  
574 heteroatoms; only 9% of detected ion abundance from gas-phase adsorbent tubes in summer and  
575 11% in winter contained a nitrogen heteroatom. This is likely due to measurement limitations;  
576 while GC-APCI techniques are extremely well-suited for the analysis of less functionalized  
577 organic compounds from both instrument transmission and ionization efficiency perspectives,  
578 these techniques are not as effective for more polar, more functionalized, more thermally-labile,  
579 or otherwise less-GC-amenable species. Thus, to examine a broader range of functionalized gas-  
580 phase compounds, we used an offline adsorptive sampling method on cooled PEEK tubing  
581 collectors and inline mobile phase desorption for LC-ESI-MS analysis (Figure 1). CH and CHS  
582 compound classes were excluded from this gas-phase LC-ESI-MS analysis due to their poor ESI  
583 ionization efficiency.

584         Due to variations in trapping and desorption effectiveness (Section S1), this method was  
585 not intended to be used as a quantitative measurement of concentration, but rather a relative  
586 assessment of the distribution of nitrogen-containing gas-phase organic compounds. The



587 variation between analytes in breakthrough testing does not influence our conclusions about the  
588 overall prevalence of observed gas-phase organic nitrogen. In laboratory tests, gas-phase sample  
589 collection, inline desorption to the mobile phase, trapping on the LC column, and  
590 chromatographic separation performed well. We observed limited breakthrough for most  
591 analytes during sampling, effective focusing prior to LC analysis, and similar separations for  
592 spiked collectors and breakthrough tests compared to standard LC runs (Figure 1B).

593 Results from the application of this new method at the YCFS revealed a wide range of  
594 compounds with oxygen-, nitrogen-, and/or sulfur-containing functionality (Figure 5) that existed  
595 at a lower average saturation mass concentration than the adsorbent tube methods during winter,  
596 with a  $\log(C_0)$  of  $3.8 \pm 2.6 \mu\text{g}/\text{m}^3$  for adsorbent tubes analyzed with GC-APCI-MS compared to  
597  $0.6 \pm 2.2 \mu\text{g}/\text{m}^3$  for functionalized gases observed via LC-ESI-MS ( $p < 0.05$ ). This decrease in  
598 volatility corresponded to an increase in the average O/C ratio of these functionalized gases to  
599  $0.2 \pm 0.2$ , which can partly be attributed to LC-ESI's poor ionization of CH compounds and to  
600 the collection system's design (targeting heteroatom-containing species and not higher volatility  
601 hydrocarbons). This may be a lower limit of O/C among functionalized compounds, as during  
602 testing with a mixture of standards, we often observed poor retention of high O/C sugars like  
603 xylitol and mannose on the LC analytical column (Table S2).

604 The gas-phase LC-ESI-MS data provide a valuable comparison to the wintertime  
605 particle-phase samples analyzed using the same instrument. These particle-phase samples had  
606 major contributions from CHO, CHON ( $O/N < 3$  and  $O/N \geq 3$ ), CHONS, and CHOS compound  
607 classes (Figure 3B). While not collected concurrently, the functionalized gas-phase samples in  
608 winter had similar contributions from CHO (20%) and CHON ( $O/N \geq 3$ ) compounds (16%),  
609 relatively more CHN (11%) and CHON ( $O/N < 3$ ) (46%) compounds, and fewer CHONS (2.7%)



610 and CHOS (4.4%) compounds (Figure 5A). The prevalence of gas-phase CHN, CHON ( $O/N <$   
611  $3$ ), and CHON ( $O/N \geq 3$ ) is of particular interest given the abundance of CHON compounds  
612 observed in the particle phase, and the potential of these gases to partition to the particle-phase  
613 and/or act as reactive precursors to other oxidized nitrogen-containing species.

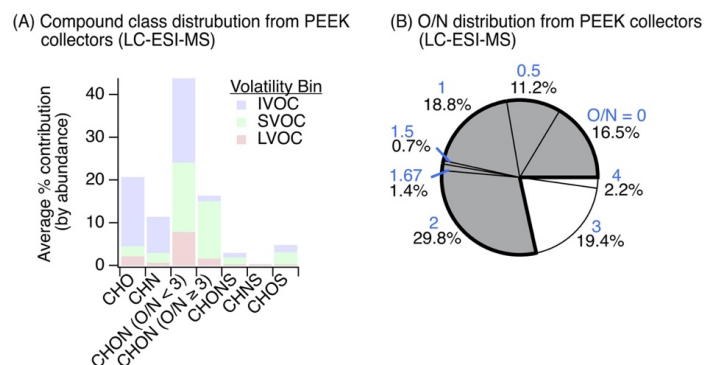
614 The presence of these nitrogen-containing compounds in the gas-phase also suggests that  
615 these compound classes observed in the particle-phase at least partly originated in the gas-phase  
616 and partitioned, rather than formed exclusively as a result of particle-phase chemistry. These  
617 species could have also formed in the particle-phase and partitioned to the gas-phase with or  
618 without condensed-phase fragmentation (discussed above). In either scenario, these nitrogen-  
619 containing compounds likely actively partitioned between phases due to their volatility (e.g.  
620 I/SVOCs shown in Figure 5A). Also, their polarity and high Henry's Law coefficients (relative  
621 to non-functionalized hydrocarbons (Sander, 2015)) suggests that these compounds could have  
622 been readily taken up by the aqueous phase. To check that these compounds were indeed gas-  
623 phase species under ambient conditions, we predicted the saturation mass concentration for  
624 individual compounds using individual ion formulas and estimated their gas-particle partitioning  
625 to a pre-existing condensed phase. While the range of compounds in Figure 5A can be expected  
626 to dynamically partition, the results confirm that the overall suite of observed compounds would  
627 have predominately existed as gases, with on average ~80% of observed ion abundance predicted  
628 to equilibrate to the gas-phase across compound classes (Figure S6).

629 Of all the gas-phase species observed with at least one nitrogen atom (i.e. CHN, CHON,  
630 CHONS, CHNS), we note that 78% of these compounds had an  $O/N$  ratio of less than 3 (Figure  
631 5B), indicating that most of these gas-phase species were not organonitrates, nitrophenols, or  
632 other similar structures. This is similar to our particle-phase results, which showed important



633 contributions from reduced nitrogen-containing groups paired with oxygen-containing groups in  
634 CHON ( $O/N < 3$ ) compounds. Notably, we observed an 11% contribution of gas-phase CHN  
635 species with this gas-phase LC-ESI-MS method (Figure 5A), in contrast to 2% CHN in the  
636 wintertime particle-phase samples (Figure 3). In the winter particle-phase samples, most CHN  
637 compounds contained amines (discussed above), and thus we postulate that these functionalized  
638 gas-phase CHN species were possibly also amines that acted as precursors to observed nitrogen-  
639 containing particle-phase compounds following oxidation and partitioning (or vice versa).

640 The substantial contribution from CHON with  $O/N < 3$  (46%) to the functionalized gas-  
641 phase samples could be linked to less photochemical processing of CHON compounds relative to  
642 the particle phase and/or the emissions/oxidation of CHN or CHON compounds. Moreover, in  
643 the particle-phase, we observed a weak negative relationship between CHN contribution and  
644 hydroxyl group prevalence in summertime measurements ( $r \sim -0.57$ ), which may support the  
645 transformation of CHN to CHON compounds via the formation of hydroxyl-containing species.



646 **Figure 5.** Observations of gas-phase nitrogen-containing compounds. (A) The distribution of  
647 functionalized gases observed via sampling on PEEK collectors ( $N = 6$ ) and inline mobile phase  
648 desorption with non-targeted LC-ESI-MS analysis contained a diversity of oxygen-, nitrogen-,  
649 and/or sulfur-containing compounds in the IVOC-LVOC range (volatility assignment and  
650 grouping was the same as discussed in Figure 2). While we cannot rule out gas-phase LVOC  
651 contributions from evaporation off of the upstream particle filter, LVOC contributions were  
652 limited ( $\sim 12\%$ ). (B) Oxygen-to-nitrogen ( $O/N$ ) ratio distribution of observed gas-phase nitrogen-  
653 containing species where  $O/N$  ratios  $< 3$  are colored grey and  $O/N$  ratios  $\geq 3$  are white (blue text  
654 above each percentage signifies the  $O/N$  ratio).



#### 655 4. Conclusions and Opportunities for Future Research

656 Together, these results suggest that a mix of direct emissions and chemical processes  
657 during summer and winter in the Long Island Sound region resulted in a diverse mixture of  
658 multifunctional gases and particles, where more than two-thirds of observed particle-phase  
659 compounds contained at least one nitrogen atom.

660 The observed nitrogen-containing functional groups existed across a range of fully  
661 reduced (e.g. amines, imines) and oxidized (e.g. nitro, organonitrate) structures. These fully  
662 reduced nitrogen functional groups were prevalent across all nitrogen-containing compound  
663 classes, including CHON species, and we highlight their importance as contributors to these  
664 multifunctional compounds beyond typical NO<sub>2</sub>-type compounds that are commonly studied  
665 using online mass spectrometers and share similar CHON molecular formulas. For instance,  
666 these gas- and particle-phase measurements of nitrogen-containing compounds are  
667 complementary to the measurements of these species made by chemical ionization mass  
668 spectrometers (CIMS) or by proton transfer reaction mass spectrometers (PTR-MS), whose  
669 ionization mechanisms can be tuned for sensitivity towards functionalized compounds of interest  
670 (Riva et al., 2019). While online mass spectrometers excel at high time resolution measurements  
671 that capture dynamic chemical processes in the atmosphere, their mass resolution is typically  
672 lower and they normally do not utilize separations, so they largely depend on parent ion mass-to-  
673 charge ratios to assign molecular formulas without structural attribution. The offline methods  
674 used here cannot match the time resolution of online techniques. However, the use of  
675 chromatography to separate isomers, longer sampling times to increase sensitivity toward a  
676 greater range of compounds, and the use of higher resolution mass spectrometers with MS/MS  
677 capabilities allow for improved compound identification and determination of functional group



678 distribution at the molecular level. This enables us to distinguish between true NO<sub>z</sub> species and  
679 those that contain combinations of nitrogen and oxygen but are not NO<sub>x</sub> oxidation products.  
680 Thus, both these online and offline methods should be employed together to differentiate a wider  
681 range of nitrogen-containing species and to achieve both temporal and chemical resolution.

682 As discussed throughout this work, the Long Island Sound region is affected by a mixture  
683 of anthropogenic, biogenic, and marine sources, all of which contain known emitters of organic  
684 nitrogen. Understanding the combined effect of these individual sources and their chemical  
685 transformations will be important in regions like the Long Island Sound, where a significant  
686 degree of mixing occurs over the Sound before air parcels arrive inland. For example, past work  
687 has noted extremely high contributions from alkylamines in biomass burning-influenced air  
688 mixed with marine air (Di Lorenzo et al., 2018). Similar enhancements could be expected when  
689 mixing other prominent sources of amines with marine air, such as in the aging urban outflow  
690 from the Central Atlantic and Northeast U.S., which may be transported up the coast and impact  
691 states in the surrounding region.

692 As with any ambient site, these mixed emissions are chemically processed in the  
693 atmosphere via a multitude of pathways. Here, we observed evidence of photochemical and  
694 aqueous processes occurring in both seasons, but in the winter we observed various mixture-wide  
695 trends that suggested an enhanced role for aqueous-phase processing. These observations  
696 included higher overall particle-phase volatility and smaller carbon backbone sizes, which may  
697 indicate a more important role for aqueous-phase fragmentation reactions or aqueous uptake of  
698 water soluble gases (Brege et al., 2018). We also observed key marker functional groups that  
699 may be formed via aqueous phase chemistry (e.g. nitrophenols, azoles). The role of aqueous-  
700 phase chemistry and aqueous-phase uptake of gases is increasingly studied in laboratory and



701 ambient contexts (Herrmann et al., 2015), and such chemistry should further examined especially  
702 in coastal and other humid regions.

703 For example, the aqueous-phase processing of atmospherically relevant nitrogen-  
704 containing species is particularly important to understand in ambient air due to the potential of  
705 brown carbon formation, which has significant impacts on climate forcing (Laskin et al., 2015).  
706 The role of ammonia and amines reacting with carbonyls is of interest for this type of chemistry  
707 (e.g. DeHaan et al., 2009; Grace et al., 2020; McNeill, 2015; Sareen et al., 2010) and should  
708 continue to be explored, particularly in coastal settings where concentrations of small gas-phase  
709 amines may be high due to their marine sources. As discussed above, our ambient observations  
710 of azoles could be indicative of such chemistry, and should be explored in future comparisons of  
711 ambient and laboratory-generated species. Also, we observed a significant contribution from  
712 nitrophenols at our site, and while they are not formed by this same chemistry, they represent  
713 another important form of light absorbing nitrogen-containing organic mass in the atmosphere  
714 (Hems and Abbatt, 2018). Finally, many of the nitrogen-containing functional groups observed  
715 in this work may be susceptible to hydrolysis, so the balance between hydrolysis and other  
716 aqueous pathways is important to consider and understand for appropriate representation of  
717 nitrogen-containing compounds in models for both aqueous aerosol and in-cloud/fog chemistry.

718 As another example, the greater prevalence of I/SVOCs observed in the winter particle-  
719 phase samples suggested possible dynamic partitioning or aqueous uptake of lighter gas-phase  
720 compounds; to explore the composition of these lighter gas-phase compounds that could exist as  
721 I/SVOCs and thus participate in phase partitioning, we supplemented our particle-phase analyses  
722 with a novel approach for investigating functionalized gases with LC-ESI-MS. Further  
723 investigation of these nitrogen-containing gases will facilitate new understanding of their gas-



724 particle partitioning in the presence of aerosol liquid water and organic condensed species, and  
725 measurements across dynamic conditions will help elucidate the relative importance of both  
726 processes. For these types of measurements, further design iterations of the PEEK sampling  
727 system for functionalized gases and additional functionalized gas-phase samples for LC-ESI-MS  
728 analysis could be pursued. Concurrent high volume filter samples could be collected for direct  
729 comparison to the particle-phase, which was not possible in this study due to insufficient mass  
730 loading on the upstream filter during the short duration functionalized gas sample (i.e. 2 hours).  
731 Concurrent PEEK samples could also be collected for MS/MS analysis.

732 In all, combinations of online and offline mass spectrometry to obtain temporal and  
733 chemical detail, further ambient observations of major organic nitrogen sources, a better  
734 understanding of the aqueous processing of nitrogen-containing compounds, and improved  
735 characterization of their gas-particle partitioning in the presence of aerosol liquid water will  
736 together allow for a more accurate representation of nitrogen-containing organic compounds in  
737 emission inventories and models, and enhance our ability to predict their impacts on atmospheric  
738 composition, human health, and climate.

739

740 **Author contributions:** J.C.D. and D.R.G. planned the field sampling and study. J.C.D. collected  
741 and analyzed field samples, and performed PEEK sampling and inline LC method development.  
742 J.M. performed inline LC method development. J.C.D. and D.R.G. wrote the manuscript with  
743 contributions from all co-authors.

744

745 **Data availability:** Data are available upon request to Drew R. Gentner

746 ([drew.gentner@yale.edu](mailto:drew.gentner@yale.edu)).

747



748 **Competing interests:** The authors declare that they have no substantive conflicts of interest but  
749 acknowledge that D.R.G. is an associate editor with *Atmospheric Chemistry and Physics*.

750

751 **Acknowledgements:** We acknowledge support from the National Science Foundation  
752 (AGS1764126) and the Yale Natural Lands Program. We also acknowledge GERSTEL for their  
753 collaboration with the thermal desorption unit used here. We thank David Wheeler at the New  
754 York Department of Environmental Conservation, Pete Babich and Adam Augustine at the  
755 Connecticut Department of Energy and Environmental Protection, Luke Valin at the  
756 Environmental Protection Agency, and Jordan Peccia at Yale for use of sampling equipment, as  
757 well as Paul Miller (NESCAUM) for organizing the LISTOS project. We also thank Richard  
758 Boardman and the Yale Peabody Museum for enabling us to set up and collect samples at the  
759 YCFS site, and acknowledge the help of Yale Peabody Museum EVOLUTIONS interns: Amir  
760 Bond, Ethan Weed, Paula Mock, and Aurea Orenca. We thank Trevor VandenBoer and Barbara  
761 Ervens for helpful feedback on the draft manuscript. Finally, we acknowledge the NOAA Air  
762 Resources Laboratory (ARL) for the provision of the HYSPLIT transport and dispersion model.

763

## 764 **References**

765

766 Borduas, N., Da Silva, G., Murphy, J. G. and Abbatt, J. P. D.: Experimental and theoretical understanding of the gas  
767 phase oxidation of atmospheric amides with OH radicals: Kinetics, products, and mechanisms, *J. Phys. Chem. A*,  
768 119(19), 4298–4308, doi:10.1021/jp503759f, 2015.

769

770 Brean, J., Dall'Osto, M., Simó, R., Shi, Z., Beddows, D. C. S. and Harrison, R. M.: Open ocean and coastal new  
771 particle formation from sulfuric acid and amines around the Antarctic Peninsula, *Nat. Geosci.*, 14(6), 383–388,  
772 doi:10.1038/s41561-021-00751-y, 2021.

773

774 Brege, M., Paglione, M., Gilardoni, S., Decesari, S., Facchini, M. C. and Mazzoleni, L. R.: Molecular insights on  
775 aging and aqueous-phase processing from ambient biomass burning emissions-influenced Po Valley fog and aerosol,  
776 *Atmos. Chem. Phys.*, 18(17), 13197–13214, doi:10.5194/acp-18-13197-2018, 2018.

777

778 Chen, C. L., Chen, S., Russell, L. M., Liu, J., Price, D. J., Betha, R., Sanchez, K. J., Lee, A. K. Y., Williams, L.,  
779 Collier, S. C., Zhang, Q., Kumar, A., Kleeman, M. J., Zhang, X. and Cappa, C. D.: Organic Aerosol Particle  
780 Chemical Properties Associated With Residential Burning and Fog in Wintertime San Joaquin Valley (Fresno) and



- 781 With Vehicle and Firework Emissions in Summertime South Coast Air Basin (Fontana), *J. Geophys. Res. Atmos.*,  
782 123(18), 10707–10731, doi:10.1029/2018JD028374, 2018.  
783
- 784 Cleveland, W. S., Kleiner, B., McRae, J. E. and Warner, J. L.: Photochemical air pollution: Transport from the New  
785 York City area into Connecticut and Massachusetts, *Science.*, 191(4223), 179–181, doi:10.1126/science.1246603,  
786 1976.  
787
- 788 Dall'Osto, M., Airs, R. L., Beale, R., Cree, C., Fitzsimons, M. F., Beddows, D., Harrison, R. M., Ceburnis, D.,  
789 O'Dowd, C., Rinaldi, M., Paglione, M., Nenes, A., Decesari, S. and Simó, R.: Simultaneous Detection of  
790 Alkylamines in the Surface Ocean and Atmosphere of the Antarctic Sympagic Environment, *ACS Earth Sp. Chem.*,  
791 3(5), 854–862, doi:10.1021/acsearthspacechem.9b00028, 2019.  
792
- 793 Decesari, S., Paglione, M., Rinaldi, M., Dall'osto, M., Simó, R., Zanca, N., Volpi, F., Cristina Facchini, M.,  
794 Hoffmann, T., Götz, S., Johannes Kampf, C., O'Dowd, C., Ceburnis, D., Ovadnevaite, J. and Tagliavini, E.:  
795 Shipborne measurements of Antarctic submicron organic aerosols: An NMR perspective linking multiple sources  
796 and bioregions, *Atmos. Chem. Phys.*, 20(7), 4193–4207, doi:10.5194/acp-20-4193-2020, 2020.  
797
- 798 DeHaan, D. O., Corrigan, A. L., Smith, K. W., Stroik, D. R., Turley, J. J., Lee, F. E., Tolbert, M. A., Jimenez, J. L.,  
799 Cordova, K. E., Ferrell, G. R., Haan, D. O. De, Corrigan, A. L., Smith, K. W., Stroik, D. R., Turley, J. J., Lee, F. E.,  
800 Tolbert, M. A., Jimenez, J. L., Cordova, K. E. and Ferrell, G. R.: Secondary organic aerosol-forming reactions of  
801 glyoxal with amino acids, *Environ. Sci. Technol.*, 43(8), 2818–2824, doi:10.1021/es803534f, 2009.  
802
- 803 Di, Q., Wang, Y., Zanobetti, A., Wang, Y., Koutrakis, P., Choirat, C., Dominici, F. and Schwartz, J. D.: Air  
804 pollution and mortality in the medicare population, *N. Engl. J. Med.*, 376(26), 2513–2522,  
805 doi:10.1056/NEJMoal702747, 2017.  
806
- 807 Ditto, J. C., Barnes, E. B., Khare, P., Takeuchi, M., Joo, T., Bui, A. A. T., Lee-Taylor, J., Eris, G., Chen, Y.,  
808 Aumont, B., Jimenez, J. L., Ng, N. L., Griffin, R. J. and Gentner, D. R.: An omnipresent diversity and variability in  
809 the chemical composition of atmospheric functionalized organic aerosol, *Commun. Chem.*, 1(1), 75,  
810 doi:10.1038/s42004-018-0074-3, 2018.  
811
- 812 Ditto, J. C., Joo, T., Khare, P., Sheu, R., Takeuchi, M., Chen, Y., Xu, W., Bui, A. A. T., Sun, Y., Ng, N. L. and  
813 Gentner, D. R.: Effects of Molecular-Level Compositional Variability in Organic Aerosol on Phase State and  
814 Thermodynamic Mixing Behavior, *Environ. Sci. Technol.*, 53(22), 13009–13018, doi:10.1021/acs.est.9b02664,  
815 2019.  
816
- 817 Ditto, J. C., Joo, T., Slade, J. H., Shepson, P. B., Ng, N. L. and Gentner, D. R.: Nontargeted Tandem Mass  
818 Spectrometry Analysis Reveals Diversity and Variability in Aerosol Functional Groups across Multiple Sites,  
819 Seasons, and Times of Day, *Environ. Sci. Technol. Lett.*, 7(2), 60–69, doi:10.1021/acs.estlett.9b00702, 2020.  
820
- 821 Ditto, J. C., He, M., Hass-Mitchell, T. N., Moussa, S. G., Hayden, K., Li, S.-M., Liggio, J., Leithead, A., Lee, P.,  
822 Wheeler, M. J., Wentzell, J. J. B. and Gentner, D. R.: Atmospheric Evolution of Emissions from a Boreal Forest  
823 Fire: The Formation of Highly-Functionalized Oxygen-, Nitrogen-, and Sulfur-Containing Compounds, *Atmos.*  
824 *Chem. Phys.*, 21, 255–267, 2021.  
825
- 826 Donahue, N. M., Epstein, S. A., Pandis, S. N. and Robinson, A. L.: A two-dimensional volatility basis set: 1.  
827 organic-aerosol mixing thermodynamics, *Atmos. Chem. Phys.*, 11(7), 3303–3318, doi:10.5194/acp-11-3303-2011,  
828 2011.  
829
- 830 Dührkop, K., Shen, H., Meusel, M., Rousu, J. and Böcker, S.: Searching molecular structure databases with tandem  
831 mass spectra using CSI:FingerID, *Proc. Natl. Acad. Sci.*, 112(41), 12580–12585, doi:10.1073/pnas.1509788112,  
832 2015.  
833
- 834 Dührkop, K., Fleischauer, M., Ludwig, M., Aksekov, A. A., Melnik, A. V., Meusel, M., Dorrestein, P. C., Rousu, J.  
835 and Böcker, S.: SIRIUS 4: a rapid tool for turning tandem mass spectra into metabolite structure information, *Nat.*  
836 *Methods*, 16(4), 299–302, doi:10.1038/s41592-019-0344-8, 2019.



- 837  
838  
839 Dunlea, E. J., Herndon, S. C., Nelson, D. D., Volkamer, R. M., San Martini, F., Sheehy, P. M., Zahniser, M. S.,  
840 Shorter, J. H., Wormhoudt, J. C., Lamb, B. K., Allwine, E. J., Gaffney, J. S., Marley, N. A., Grutter, M., Marquez,  
841 C., Blanco, S., Cardenas, B., Retama, A., Ramos Villegas, C. R., Kolb, C. E., Molina, L. T. and Molina, M. J.:  
842 Evaluation of nitrogen dioxide chemiluminescence monitors in a polluted urban environment, *Atmos. Chem. Phys.*,  
843 7(10), 2691–2704, doi:10.5194/acp-7-2691-2007, 2007.
- 844  
845 Ervens, B., Turpin, B. J. and Weber, R. J.: Secondary organic aerosol formation in cloud droplets and aqueous  
846 particles (aqSOA): A review of laboratory, field and model studies, *Atmos. Chem. Phys.*, 11(21), 11069–11102,  
847 doi:10.5194/acp-11-11069-2011, 2011.
- 848  
849 Gaston, C. J., Quinn, P. K., Bates, T. S., Gilman, J. B., Bon, D. M., Kuster, W. C. and Prather, K. A.: The impact of  
850 shipping, agricultural, and urban emissions on single particle chemistry observed aboard the R/V Atlantis during  
851 CalNex, *J. Geophys. Res. Atmos.*, 118(10), 5003–5017, doi:10.1002/jgrd.50427, 2013.
- 852  
853 Ge, X., Wexler, A. S. and Clegg, S. L.: Atmospheric amines - Part I. A review, *Atmos. Environ.*, 45(3), 524–546,  
854 doi:10.1016/j.atmosenv.2010.10.012, 2011.
- 855  
856 Ge, Y., Liu, Y., Chu, B., He, H., Chen, T., Wang, S., Wei, W. and Cheng, S.: Ozonolysis of Trimethylamine  
857 Exchanged with Typical Ammonium Salts in the Particle Phase, *Environ. Sci. Technol.*, 50(20), 11076–11084,  
858 doi:10.1021/acs.est.6b04375, 2016.
- 859  
860 de Gouw, J. A., Middlebrook, A. M., Warneke, C., Goldan, P. D., Kuster, W. C., Roberts, J. M., Fehsenfeld, F. C.,  
861 Worsnop, D. R., Canagaratna, M. R., Pszenny, A. A. P., Keene, W. C., Marchewka, M., Bertman, S. B. and Bates,  
862 T. S.: Budget of organic carbon in a polluted atmosphere: Results from the New England Air Quality Study in 2002,  
863 *J. Geophys. Res. D Atmos.*, 110(16), 1–22, doi:10.1029/2004JD005623, 2005.
- 864  
865 Grace, D. N., Sharp, J. R., Holappa, R. E., Lugos, E. N., Sebold, M. B., Griffith, D. R., Hendrickson, H. P. and  
866 Galloway, M. M.: Heterocyclic Product Formation in Aqueous Brown Carbon Systems, *ACS Earth Sp. Chem.*,  
867 3(11), 2472–2481, doi:10.1021/acsearthspacechem.9b00235, 2019.
- 868  
869 Grace, D. N., Lugos, E. N., Ma, S., Griffith, D. R., Hendrickson, H. P., Woo, J. L. and Galloway, M. M.: Brown  
870 Carbon Formation Potential of the Biacetyl-Ammonium Sulfate Reaction System, *ACS Earth Sp. Chem.*, 4(7),  
871 1104–1113, doi:10.1021/acsearthspacechem.0c00096, 2020.
- 872  
873 Hallquist, M., Wenger, J. C., Baltensperger, U., Rudich, Y., Simpson, D., Claeys, M., Dommen, J., Donahue, N. M.,  
874 George, C., Goldstein, A. H., Hamilton, J. F., Herrmann, H., Hoffmann, T., Iinuma, Y., Jang, M., Jenkin, M. E.,  
875 Jimenez, J. L., Kiendler-Scharr, A., Maenhaut, W., McFiggans, G., Mentel, T. F., Monod, A., Prevot, A. S. H.,  
876 Seinfeld, J. H., Surratt, J. D., Szmigielski, R. and Wildt, J.: The formation, properties and impact of secondary  
877 organic aerosol: current and emerging issues, *Atmos. Chem. Phys.*, 9(14), 5155–5236, doi:10.5194/acp-9-5155-  
878 2009, 2009.
- 879  
880 Hems, R. F. and Abbatt, J. P. D.: Aqueous Phase Photo-oxidation of Brown Carbon Nitrophenols: Reaction  
881 Kinetics, Mechanism, and Evolution of Light Absorption, *ACS Earth Sp. Chem.*, 2(3), 225–234,  
882 doi:10.1021/acsearthspacechem.7b00123, 2018.
- 883  
884 Herrmann, H., Schaefer, T., Tilgner, A., Styler, S. A., Weller, C., Teich, M. and Otto, T.: Tropospheric Aqueous-  
885 Phase Chemistry: Kinetics, Mechanisms, and Its Coupling to a Changing Gas Phase, *Chem. Rev.*, 115(10), 4259–  
886 4334, doi:10.1021/cr500447k, 2015.
- 887  
888 Jerrett, M., Burnett, R. T., Pope, C. A., Ito, K., Thurston, G., Krewski, D., Shi, Y., Calle, E. and Thun, M.: Long-  
889 term ozone exposure and mortality, *N. Engl. J. Med.*, 360(11), 1085–1095, doi:10.1056/NEJMoa0803894, 2009.
- 890  
891 Juncosa Calahorrano, J. F., Lindaas, J., O'Dell, K., Palm, B. B., Peng, Q., Flocke, F., Pollack, I. B., Garofalo, L. A.,  
892 Farmer, D. K., Pierce, J. R., Collett, J. L., Weinheimer, A., Campos, T., Hornbrook, R. S., Hall, S. R., Ullmann, K.,  
Pothier, M. A., Apel, E. C., Permar, W., Hu, L., Hills, A. J., Montzka, D., Tyndall, G., Thornton, J. A. and Fischer,



- 893 E. V.: Daytime Oxidized Reactive Nitrogen Partitioning in Western U.S. Wildfire Smoke Plumes, *J. Geophys. Res.*  
894 *Atmos.*, 126(4), 1–22, doi:10.1029/2020JD033484, 2021.
- 895
- 896 Khare, P. and Gentner, D. R.: Considering the future of anthropogenic gas-phase organic compound emissions and  
897 the increasing influence of non-combustion sources on urban air quality, *Atmos. Chem. Phys.*, 18(8), 5391–5413,  
898 doi:10.5194/acp-18-5391-2018, 2018.
- 899
- 900 Khare, P., Marcotte, A., Sheu, R., Walsh, A. N., Ditto, J. C. and Gentner, D. R.: Advances in offline approaches for  
901 trace measurements of complex organic compound mixtures via soft ionization and high-resolution tandem mass  
902 spectrometry, *J. Chromatogr. A*, 1598, 163–174, doi:10.1016/j.chroma.2019.03.037, 2019.
- 903
- 904 Kieloaho, A. J., Hellén, H., Hakola, H., Manninen, H. E., Nieminen, T., Kulmala, M. and Pihlatie, M.: Gas-phase  
905 alkylamines in a boreal Scots pine forest air, *Atmos. Environ.*, 80, 369–377, doi:10.1016/j.atmosenv.2013.08.019,  
906 2013.
- 907
- 908 Kilian, J. and Kitazawa, M.: The emerging risk of exposure to air pollution on cognitive decline and Alzheimer’s  
909 disease – Evidence from epidemiological and animal studies, *Biomed. J.*, 41(3), 141–162,  
910 doi:10.1016/j.bj.2018.06.001, 2018.
- 911
- 912 Laskin, A., Laskin, J. and Nizkorodov, S. A.: Chemistry of Atmospheric Brown Carbon, *Chem. Rev.*, 115(10),  
913 4335–4382, doi:10.1021/cr5006167, 2015.
- 914
- 915 Leslie, M. D., Ridoli, M., Murphy, J. G. and Borduas-Dedekind, N.: Isocyanic acid (HNCO) and its fate in the  
916 atmosphere: A review, *Environ. Sci. Process. Impacts*, 21(5), 793–808, doi:10.1039/c9em00003h, 2019.
- 917
- 918 Li, Y., Pöschl, U. and Shiraiwa, M.: Molecular corridors and parameterizations of volatility in the chemical  
919 evolution of organic aerosols, *Atmos. Chem. Phys.*, 16(5), 3327–3344, doi:10.5194/acp-16-3327-2016, 2016.
- 920
- 921 Liebmann, J., Sobanski, N., Schuladen, J., Karu, E., Hellén, H., Hakola, H., Zha, Q., Ehn, M., Riva, M., Heikkinen,  
922 L., Williams, J., Fischer, H., Lelieveld, J. and Crowley, J. N.: Alkyl nitrates in the boreal forest: formation via the  
923 NO<sub>3</sub>-, OH- and O<sub>3</sub>-induced oxidation of biogenic volatile organic compounds and ambient lifetimes, *Atmos. Chem.*  
924 *Phys.*, 19, 10391–10403, doi:10.5194/acp-2019-463, 2019.
- 925
- 926 Lim, S., McArdell, C. S. and von Gunten, U.: Reactions of aliphatic amines with ozone: Kinetics and mechanisms,  
927 *Water Res.*, 157, 514–528, doi:10.1016/j.watres.2019.03.089, 2019.
- 928
- 929 Lim, Y. Bin, Kim, H., Kim, J. Y. and Turpin, B. J.: Photochemical organonitrate formation in wet aerosols, *Atmos.*  
930 *Chem. Phys.*, 16(19), 12631–12647, doi:10.5194/acp-16-12631-2016, 2016.
- 931
- 932 Lin, P., Laskin, J., Nizkorodov, S. A. and Laskin, A.: Revealing Brown Carbon Chromophores Produced in  
933 Reactions of Methylglyoxal with Ammonium Sulfate, *Environ. Sci. Technol.*, 49(24), 14257–14266,  
934 doi:10.1021/acs.est.5b03608, 2015.
- 935
- 936 Di Lorenzo, R. A., Place, B. K., VandenBoer, T. C. and Young, C. J.: Composition of Size-Resolved Aged Boreal  
937 Fire Aerosols: Brown Carbon, Biomass Burning Tracers, and Reduced Nitrogen, *ACS Earth Sp. Chem.*, 2(3), 278–  
938 285, doi:10.1021/acsearthspacechem.7b00137, 2018.
- 939
- 940 Loza, C. L., Craven, J. S., Yee, L. D., Coggon, M. M., Schwantes, R. H., Shiraiwa, M., Zhang, X., Schilling, K. A.,  
941 Ng, N. L., Canagaratna, M. R., Ziemann, P. J., Flagan, R. C. and Seinfeld, J. H.: Secondary organic aerosol yields of  
942 12-carbon alkanes, *Atmos. Chem. Phys.*, 14(3), 1423–1439, doi:10.5194/acp-14-1423-2014, 2014.
- 943
- 944 McNeill, V. F.: Aqueous organic chemistry in the atmosphere: Sources and chemical processing of organic aerosols,  
945 *Environ. Sci. Technol.*, 49(3), 1237–1244, doi:10.1021/es5043707, 2015.
- 946
- 947 Ng, N. L., Brown, S. S., Archibald, A. T., Atlas, E., Cohen, R. C., Crowley, J. N., Day, D. A., Donahue, N. M., Fry,  
948 J. L., Fuchs, H., Griffin, R. J., Guzman, M. I., Herrmann, H., Hodzic, A., Iinuma, Y., Kiendler-Scharr, A., Lee, B.



- 949 H., Luecken, D. J., Mao, J., McLaren, R., Mutzel, A., Osthoff, H. D., Ouyang, B., Picquet-Varrault, B., Platt, U.,  
950 Pye, H. O. T., Rudich, Y., Schwantes, R. H., Shiraiwa, M., Stutz, J., Thornton, J. A., Tilgner, A., Williams, B. J. and  
951 Zaveri, R. A.: Nitrate radicals and biogenic volatile organic compounds: oxidation, mechanisms, and organic  
952 aerosol, *Atmos. Chem. Phys.*, 17(3), 2103–2162, doi:10.5194/acp-17-2103-2017, 2017.  
953  
954 Perring, A. E., Pusede, S. E. and Cohen, R. C.: An Observational Perspective on the Atmospheric Impacts of Alkyl  
955 and Multifunctional Nitrates on Ozone and Secondary Organic Aerosol, *Chem. Rev.*, 113(8), 5848–5870,  
956 doi:10.1021/cr300520x, 2013.  
957  
958 van Pinxteren, M., Müller, C., Iinuma, Y., Stolle, C. and Herrmann, H.: Chemical Characterization of Dissolved  
959 Organic Compounds from Coastal Sea Surface Microlayers (Baltic Sea, Germany), *Environ. Sci. Technol.*, 46(19),  
960 10455–10462, doi:10.1021/es204492b, 2012.  
961  
962 van Pinxteren, M., Fomba, K. W., van Pinxteren, D., Triesch, N., Hoffmann, E. H., Cree, C. H. L., Fitzsimons, M.  
963 F., von Tümpling, W. and Herrmann, H.: Aliphatic amines at the Cape Verde Atmospheric Observatory:  
964 Abundance, origins and sea-air fluxes, *Atmos. Environ.*, 203, 183–195, doi:10.1016/j.atmosenv.2019.02.011, 2019.  
965  
966 Pope, C. A. and Dockery, D. D.: Health Effects of Fine Particulate Air Pollution: Lines that Connect, *J. Air Waste  
967 Manage. Assoc.*, 56, 709–742, doi:10.1080/10473289.2006.10464485, 2006.  
968  
969 Priestley, M., Le Breton, M., Bannan, T. J., Leather, K. E., Bacak, A., Reyes-Villegas, E., De Vocht, F., Shallcross,  
970 B. M. A., Brazier, T., Khan, M. A., Allan, J., Shallcross, D. E., Coe, H. and Percival, C. J.: Observations of  
971 Isocyanate, Amide, Nitrate, and Nitro Compounds From an Anthropogenic Biomass Burning Event Using a ToF-  
972 CIMS, *J. Geophys. Res. Atmos.*, 123, 7687–7704, doi:10.1002/2017JD027316, 2018.  
973  
974 Quinn, P. K., Collins, D. B., Grassian, V. H., Prather, K. A. and Bates, T. S.: Chemistry and Related Properties of  
975 Freshly Emitted Sea Spray Aerosol, *Chem. Rev.*, 115(10), 4383–4399, doi:10.1021/cr500713g, 2015.  
976  
977 Riva, M., Rantala, P., Krechmer, J. E., Peräkylä, O., Zhang, Y., Heikkinen, L., Garmash, O., Yan, C., Kulmala, M.,  
978 Worsnop, D. and Ehn, M.: Evaluating the performance of five different chemical ionization techniques for detecting  
979 gaseous oxygenated organic species, *Atmos. Meas. Tech.*, 12, 2403–2421, doi:https://doi.org/10.5194/amt-12-2403-  
980 2019, 2019.  
981  
982 Roberts, J. M., Veres, P. R., VandenBoer, T. C., Warneke, C., Graus, M., Williams, E. J., Lefter, B., Brock, C. A.,  
983 Bahreini, R., Ozturk, F., Middlebrook, A. M., Wagner, N. L., Dube, W. P. and DeGouw, J. A.: New insights into  
984 atmospheric sources and sinks of isocyanic acid, HNCO, from recent urban and regional observations, *J. Geophys.  
985 Res. Atmos.*, 119, 1060–1072, doi:10.1002/2013JD019931, 2014.  
986  
987 Rogers, H. M., Ditto, J. C. and Gentner, D. R.: Evidence for impacts on surface-level air quality in the northeastern  
988 US from long-distance transport of smoke from North American fires during the Long Island Sound Tropospheric  
989 Ozone Study (LISTOS) 2018, *Atmos. Chem. Phys.*, 20(2), 671–682, doi:10.5194/acp-20-671-2020, 2020.  
990  
991 Sander, R.: Compilation of Henry's law constants (version 4.0) for water as solvent, *Atmos. Chem. Phys.*, 15(8),  
992 4399–4981, doi:10.5194/acp-15-4399-2015, 2015.  
993  
994 Sareen, N., Schwier, A. N., Shapiro, E. L., Mitroo, D. and McNeill, V. F.: Secondary organic material formed by  
995 methylglyoxal in aqueous aerosol mimics, *Atmos. Chem. Phys.*, 10, 997–1016, doi:10.5194/acpd-9-15567-2009,  
996 2010.  
997  
998 Schervish, M. and Donahue, N. M.: Peroxy radical chemistry and the volatility basis set, *Atmos. Chem. Phys.*,  
999 20(2), 1183–1199, doi:10.5194/acp-20-1183-2020, 2020.  
1000  
1001 Schroder, J. C., Campuzano-Jost, P., Day, D. A., Shah, V., Larson, K., Sommers, J. M., Sullivan, A. P., Campos, T.,  
1002 Reeves, J. M., Hills, A., Hornbrook, R. S., Blake, N. J., Scheuer, E., Guo, H., Fibiger, D. L., McDuffie, E. E., Hayes,  
1003 P. L., Weber, R. J., Dibb, J. E., Apel, E. C., Jaeglé, L., Brown, S. S., Thornton, J. A. and Jimenez, J. L.: Sources and  
1004 Secondary Production of Organic Aerosols in the Northeastern United States during WINTER, *J. Geophys. Res.*



- 1005 Atmos., 123(14), 7771–7796, doi:10.1029/2018JD028475, 2018.  
1006  
1007 Sheu, R., Marcotte, A., Khare, P., Charan, S., Ditto, J. C. and Gentner, D. R.: Advances in offline approaches for  
1008 chemically speciated measurements of trace gas-phase organic compounds via adsorbent tubes in an integrated  
1009 sampling-to-analysis system, *J. Chromatogr. A*, 1575, 80–90, doi:10.1016/j.chroma.2018.09.014, 2018.  
1010 Sintermann, J. and Neftel, A.: Ideas and perspectives: On the emission of amines from terrestrial vegetation in the  
1011 context of new atmospheric particle formation, *Biogeosciences*, 12(11), 3225–3240, doi:10.5194/bg-12-3225-2015,  
1012 2015.  
1013  
1014 Sodeman, D. A., Toner, S. M. and Prather, K. A.: Determination of Single Particle Mass Spectral Signatures from  
1015 Light-Duty Vehicle Emissions, *Environ. Sci. Technol.*, 39(12), 4569–4580, doi:10.1016/j.atmosenv.2007.01.025,  
1016 2005.  
1017  
1018 Sullivan, A. P., Guo, H., Schroder, J. C., Campuzano-Jost, P., Jimenez, J. L., Campos, T., Shah, V., Jaeglé, L., Lee,  
1019 B. H., Lopez-Hilfiker, F. D., Thornton, J. A., Brown, S. S. and Weber, R. J.: Biomass Burning Markers and  
1020 Residential Burning in the WINTER Aircraft Campaign, *J. Geophys. Res. Atmos.*, 124(3), 1846–1861,  
1021 doi:10.1029/2017JD028153, 2019.  
1022  
1023 Takeuchi, M. and Ng, N. L.: Organic nitrates and secondary organic aerosol (SOA) formation from oxidation of  
1024 biogenic volatile organic compounds, *ACS Symp. Ser. Multiph. Environ. Chem. Atmos.*, 1299, 105–125,  
1025 doi:10.1021/bk-2018-1299.ch006, 2018.  
1026  
1027 Tao, Y., Liu, T., Yang, X. and Murphy, J. G.: Kinetics and Products of the Aqueous Phase Oxidation of  
1028 Triethylamine by OH, *ACS Earth Sp. Chem.*, 5(8), 1889–1895, doi:10.1021/acsearthspacechem.1c00162, 2021.  
1029  
1030 United States Environmental Protection Agency: Historical Exceedance Days in New England, Reg. 1 EPA New  
1031 Engl. [online] Available from: <https://www3.epa.gov/region1/airquality/standard.html> (Accessed 14 August 2021),  
1032 2020.  
1033  
1034 VandenBoer, T. C., Petroff, A., Markovic, M. Z. and Murphy, J. G.: Size distribution of alkyl amines in continental  
1035 particulate matter and their online detection in the gas and particle phase, *Atmos. Chem. Phys.*, 11(9), 4319–4332,  
1036 doi:10.5194/acp-11-4319-2011, 2011.  
1037  
1038 Vidović, K., Lašič Jurković, D., Šala, M., Kroflič, A. and Grgić, I.: Nighttime Aqueous-Phase Formation of  
1039 Nitrocatechols in the Atmospheric Condensed Phase, *Environ. Sci. Technol.*, 52(17), 9722–9730,  
1040 doi:10.1021/acs.est.8b01161, 2018.  
1041  
1042 Warneke, C., McKeen, S. A., de Gouw, J. A., Goldan, P. D., Kuster, W. C., Holloway, J. S., Williams, E. J., Lerner,  
1043 B. M., Parrish, D. D., Trainer, M., Fehsenfeld, F. C., Kato, S., Atlas, E. L., Baker, A. and Blake, D. R.:  
1044 Determination of urban volatile organic compound emission ratios and comparison with an emissions database, *J.*  
1045 *Geophys. Res. Atmos.*, 112(10), 1–13, doi:10.1029/2006JD007930, 2007.  
1046  
1047 Wu, C., Wen, Y., Hua, L., Jiang, J., Xie, Y., Cao, Y., Chai, S., Hou, K. and Li, H.: Rapid and highly sensitive  
1048 measurement of trimethylamine in seawater using dynamic purge-release and dopant-assisted atmospheric pressure  
1049 photoionization mass spectrometry, *Anal. Chim. Acta*, 1137, 56–63, doi:10.1016/j.aca.2020.08.060, 2020.  
1050  
1051 Ye, C., Zhou, X., Pu, D., Stutz, J., Festa, J., Spolaor, M., Tsai, C., Cantrell, C., Mauldin, R. L., Campos, T.,  
1052 Weinheimer, A., Hornbrook, R. S., Apel, E. C., Guenther, A., Kaser, L., Yuan, B., Karl, T., Haggerty, J., Hall, S.,  
1053 Ullmann, K., Smith, J. N., Ortega, J. and Knote, C.: Rapid cycling of reactive nitrogen in the marine boundary layer,  
1054 *Nature*, 532, 489–491, doi:10.1038/nature17195, 2016.  
1055  
1056 Youn, J. S., Crosbie, E., Maudlin, L. C., Wang, Z. and Sorooshian, A.: Dimethylamine as a major alkyl amine  
1057 species in particles and cloud water: Observations in semi-arid and coastal regions, *Atmos. Environ.*, 122, 250–258,  
1058 doi:10.1016/j.atmosenv.2015.09.061, 2015.  
1059  
1060 Zhang, J., Ninneman, M., Joseph, E., Schwab, M. J., Shrestha, B. and Schwab, J. J.: Mobile Laboratory



- 1061 Measurements of High Surface Ozone Levels and Spatial Heterogeneity During LISTOS 2018: Evidence for Sea  
1062 Breeze Influence, *J. Geophys. Res. Atmos.*, 125(11), 1–12, doi:10.1029/2019JD031961, 2020.  
1063  
1064 Zhou, S., Collier, S., Xu, J., Mei, F., Wang, J., Lee, Y.-N., Sedlacek, A. J., Springston, S. R., Sun, Y. and Zhang, Q.:  
1065 Influences of upwind emission sources and atmospheric processing on aerosol chemistry and properties at a rural  
1066 location in the Northeastern U.S., *J. Geophys. Res. Atmos.*, 121(10), 6049–6065, doi:10.1002/2015JD024568, 2016.  
1067